Lecture 3. Global models: Towards modeling plate tectonics

- Global surface observations
- Modes of mantle convection
- Major ingredients of plate tectonics
- Linking mantle convection and lithospheric deformations

Spherical harmonic expansion

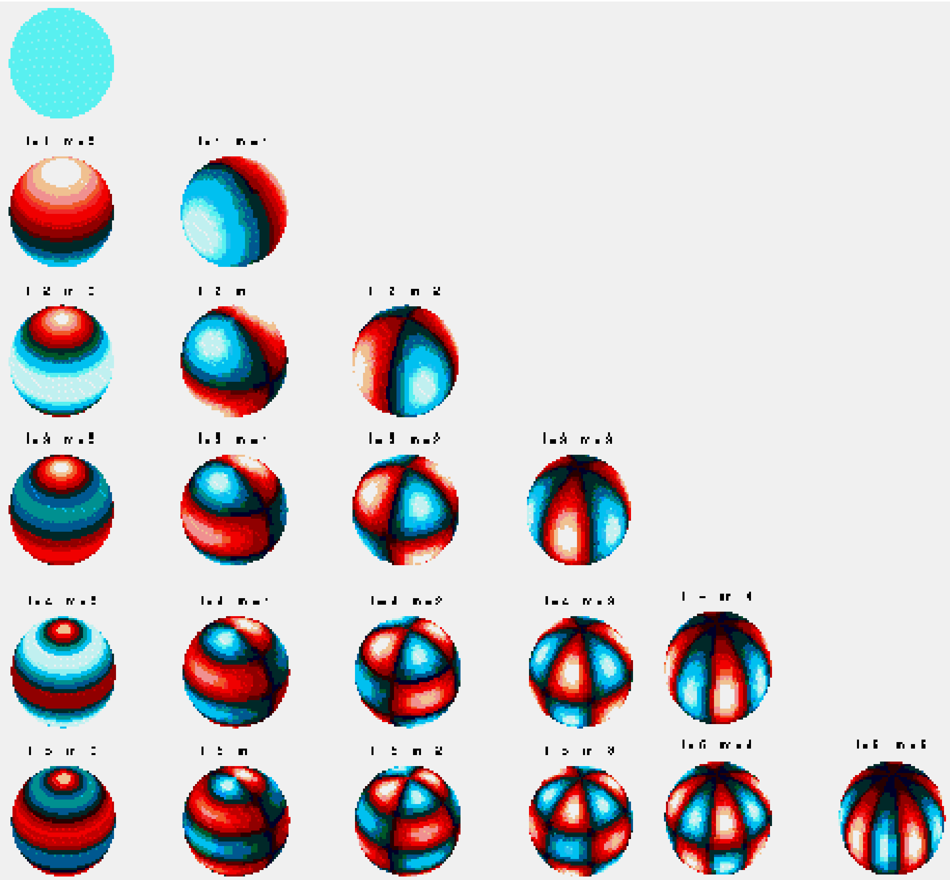

$$f(\Omega) = \sum_{l=0}^{\infty} \sum_{m=-l}^{l} f_{lm} Y_{lm}(\Omega),$$

$$Y_{lm}(\Omega) = \begin{cases} \bar{P}_{lm}(\cos\theta)\cos m\phi & \text{if } m \geq 0 \\ \bar{P}_{l|m|}(\cos\theta)\sin|m|\phi & \text{if } m < 0, \end{cases} \quad (2)$$

where the normalized associated Legendre functions are given by

$$\bar{P}_{lm}(\mu) = \sqrt{(2-\delta_{0m})(2l+1)\frac{(l-m)!}{(l+m)!}}\, P_{lm}(\mu), \quad (3)$$

and where δ_{ij} is the Kronecker delta function. The unnormalized Legendre functions in the above equation are defined in relation to the Legendre Polynomials by

$$P_{lm}(\mu) = (1-\mu^2)^{m/2} \frac{d^m}{d\mu^m} P_l(\mu), \quad (4)$$

$$P_l(\mu) = \frac{1}{2^l l!} \frac{d^l}{d\mu^l} \left(\mu^2 - 1\right)^l. \quad (5)$$

Modified from website
Of Svetlana Panasyuk

Spherical Harmonics

Example Components for Degree (L) = 8

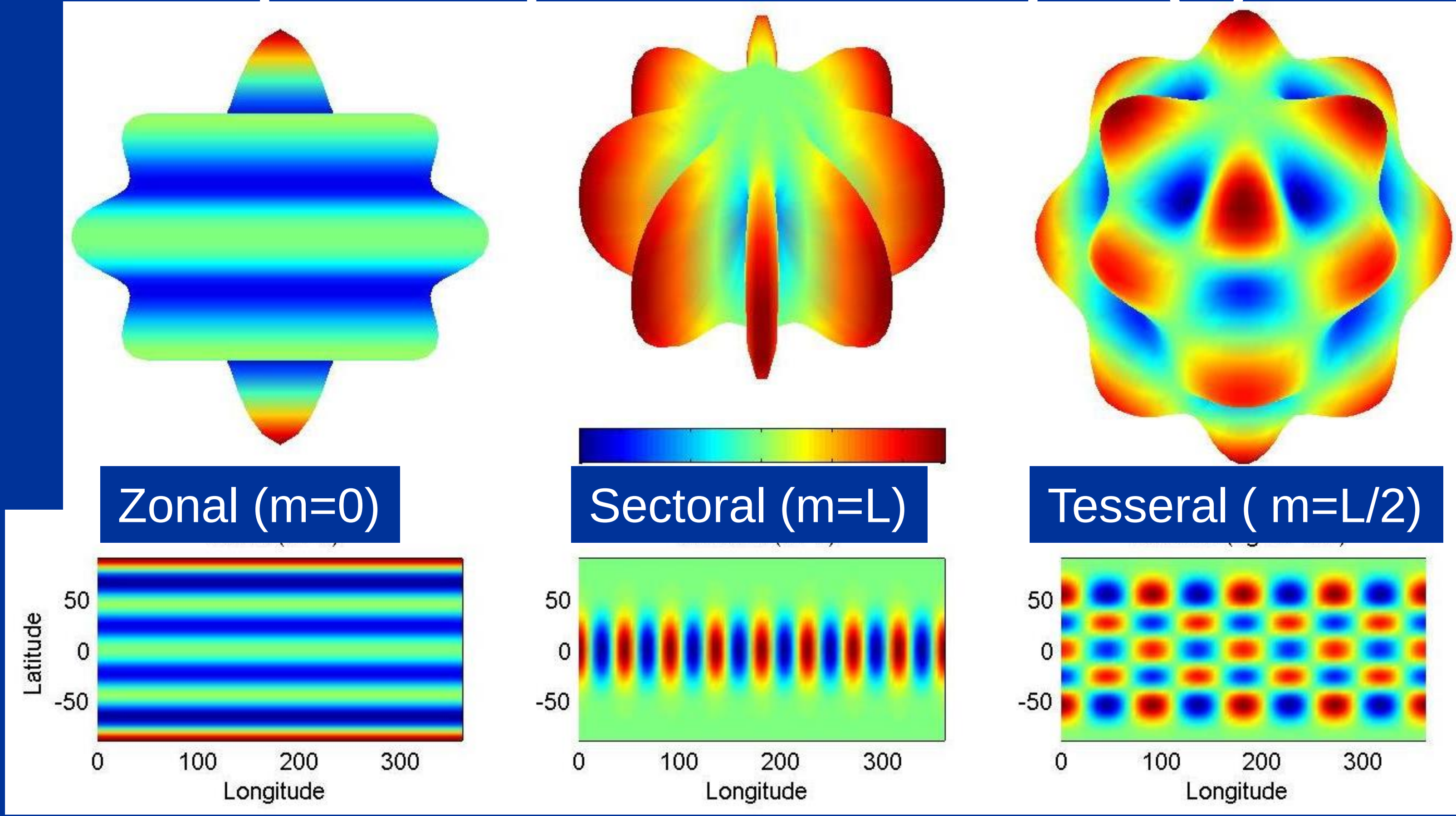

Geoid

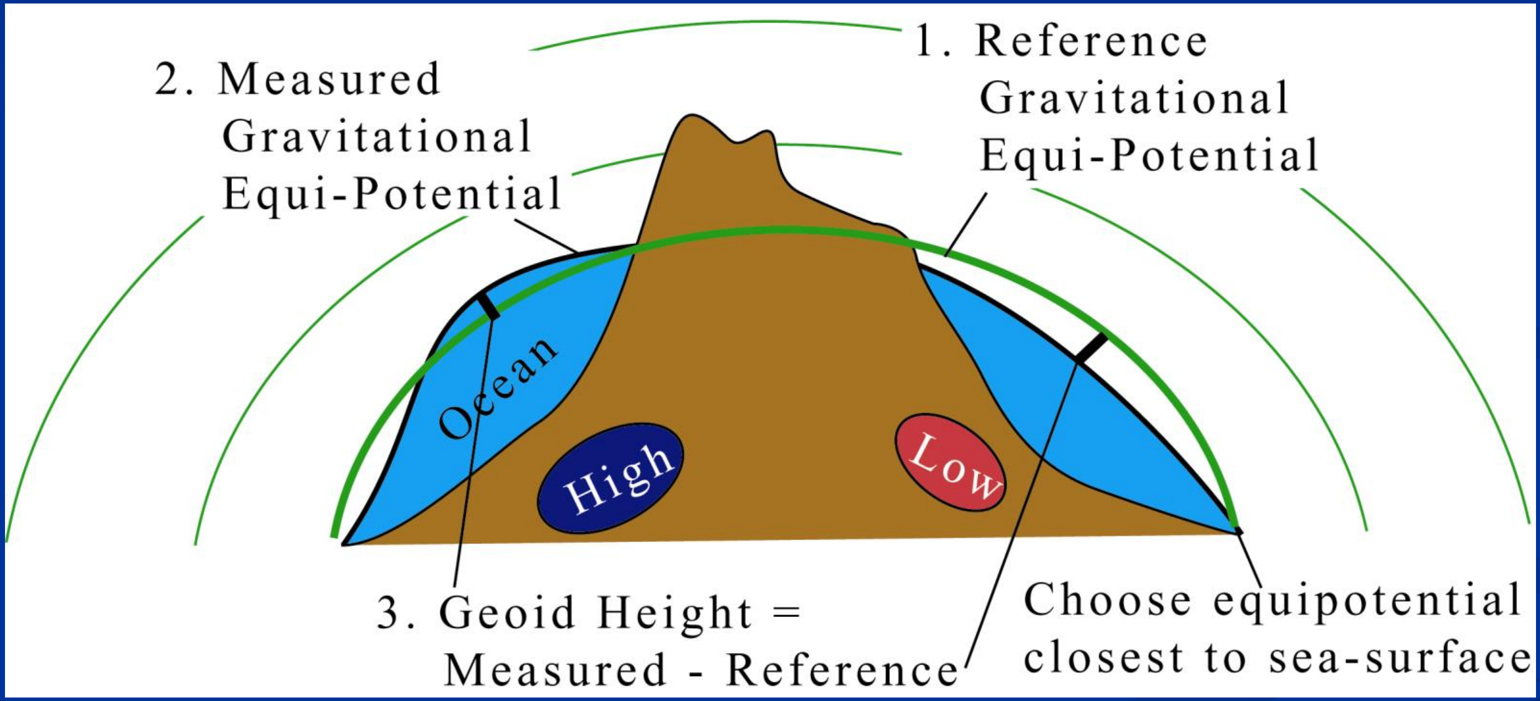

1. Reference
Gravitational
Equi-Potential
2. Measured
Gravitational
Equi-Potential
Ocean
High
Low
3. Geoid Height =
Measured - Reference
Choose equipotential
closest to sea-surface

Geoid

- Measured by modelling satellite orbits.
  - Spherical harmonic representation, L=360.

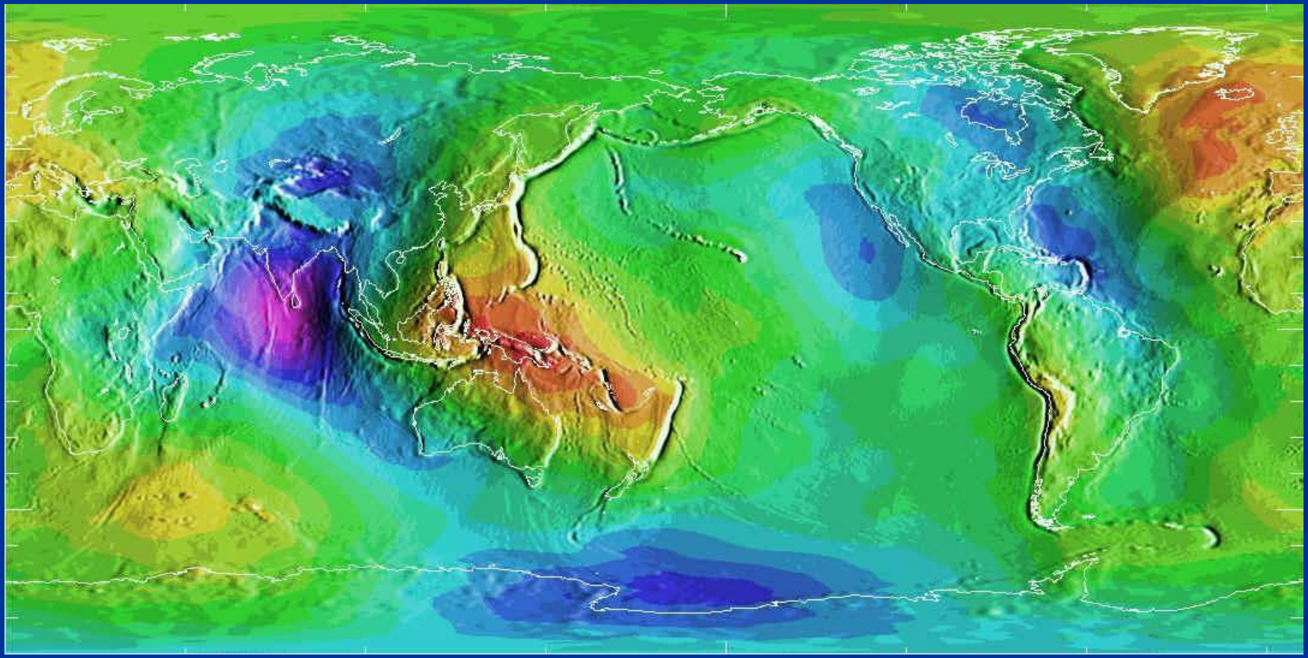

Range +/- 120 meters

From, http://www.vuw.ac.nz/scps-students/phys209/modules/mod8.htm

Free-Air Gravity

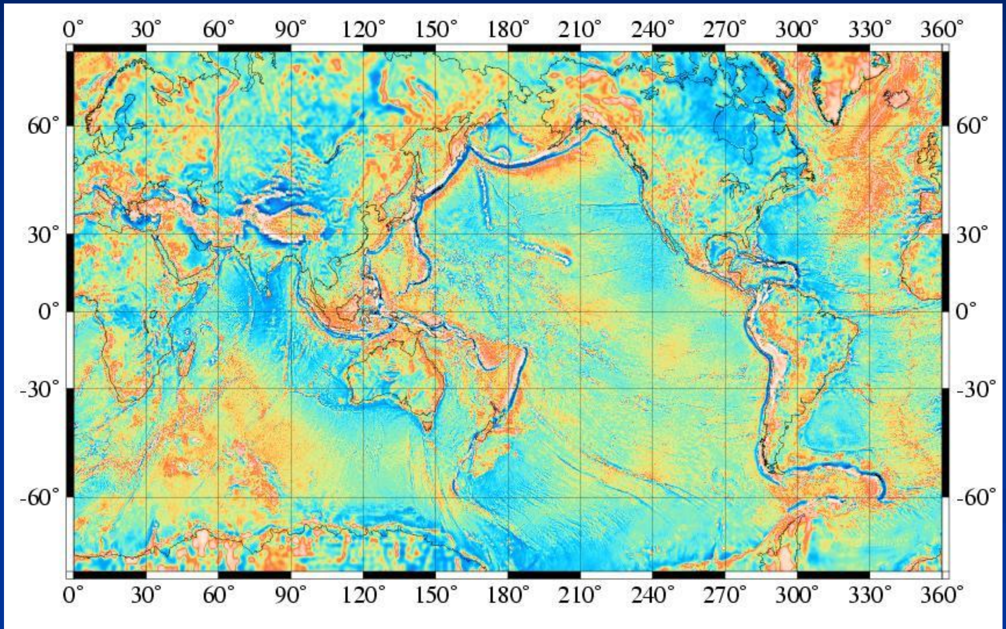

- Derivative of geoid (continents)
- Measured over the oceans using satellite altimetry (higher resolution).

Free-Air Gravity

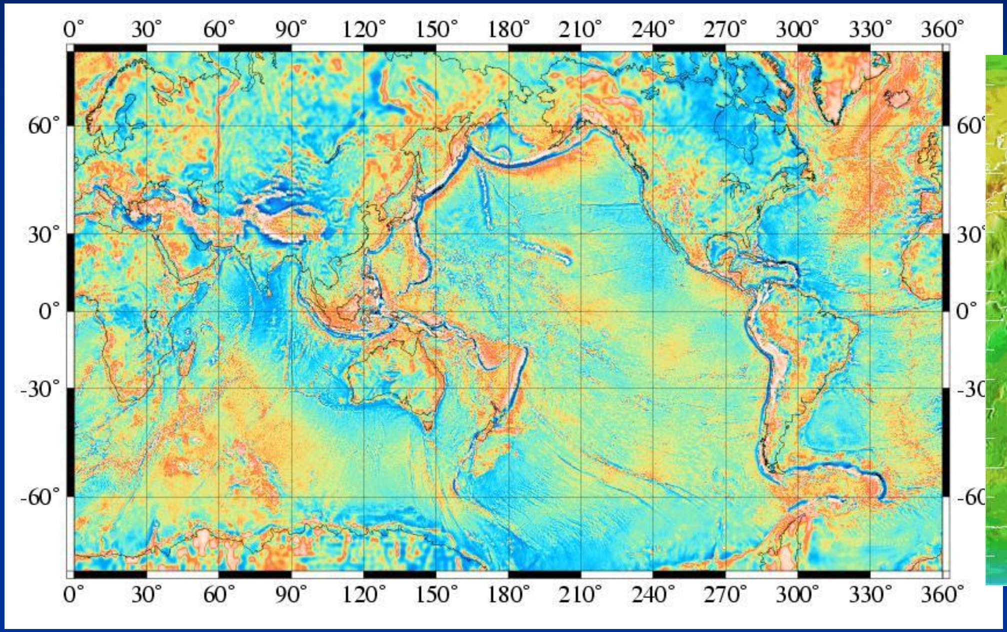

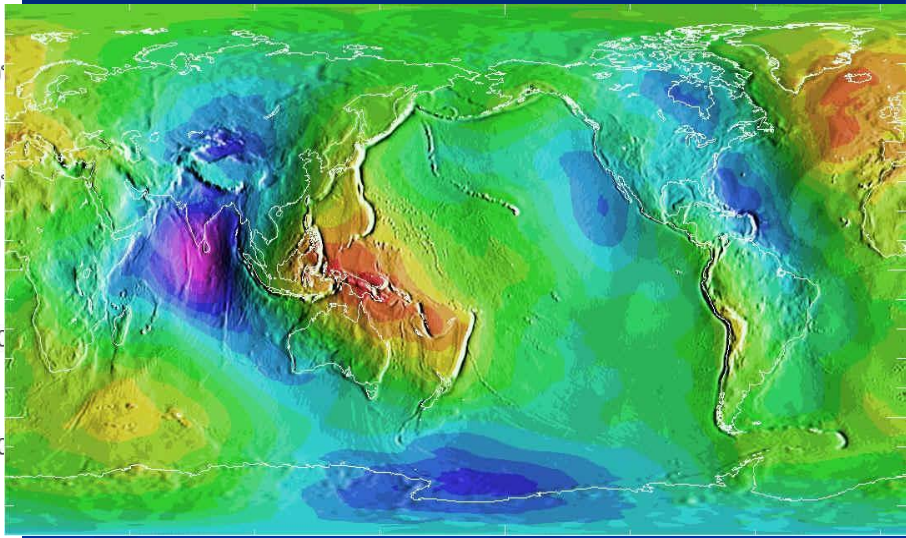

- Derivative of geoid (continents)
- Measured over the oceans using satellite altimetry (higher resolution).

Geoid/Free-air Gravity Spectra

Red Spectrum
Dominated by signal at long wavelengths

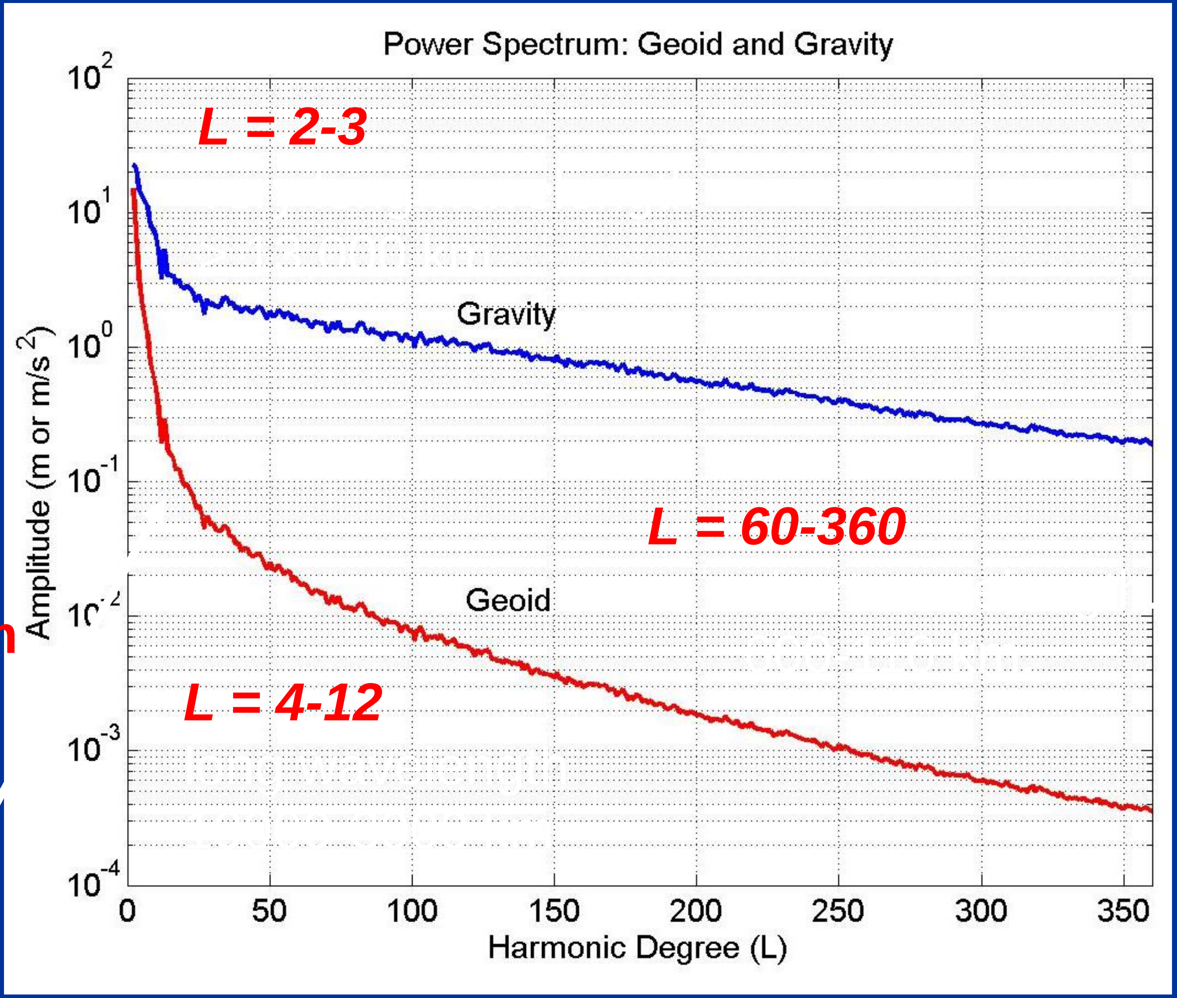

Dynamic Topography

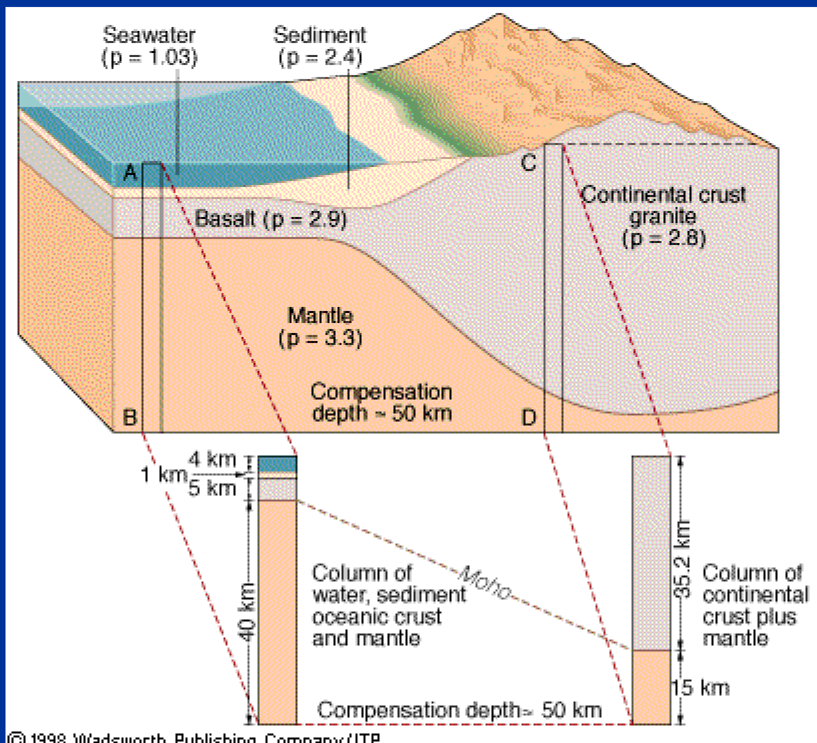

Isostatically Compensated

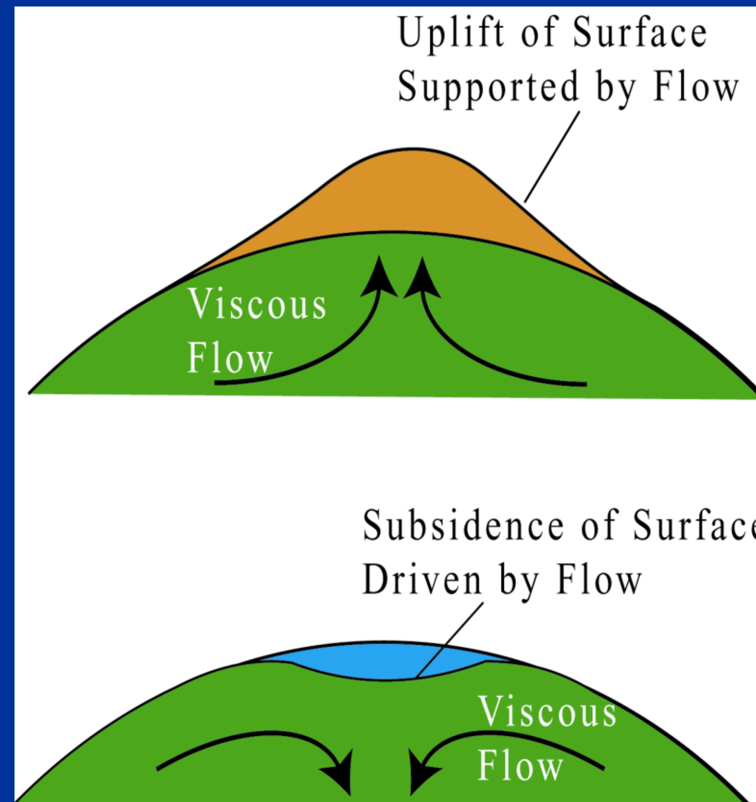

Dynamically Supported

Post-Glacial Rebound (PGR)

- Glacial Isostatic Adjustment (GIA).
  - ***returning to isostatic equilibrium***.
  - Unloading of the surface as ice melts (rapidly).

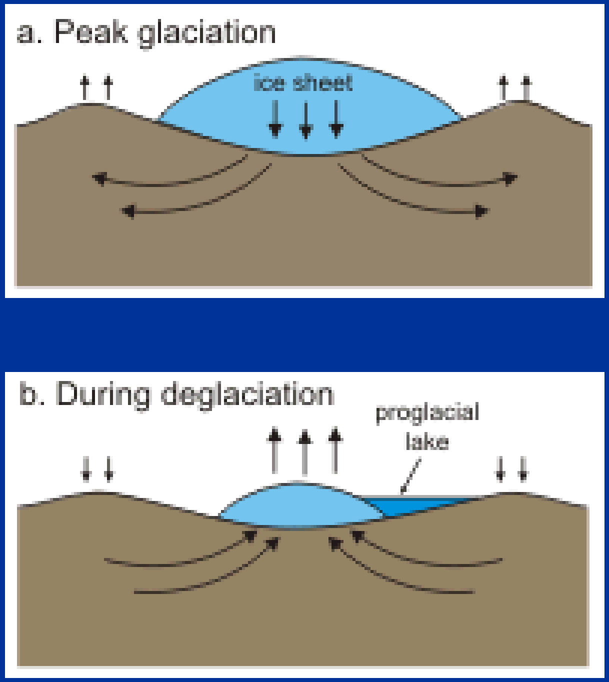

From: http://www.pgc.nrcan.gc.ca/geodyn/docs/rebound/glacial.html

Plate Motion

- Well-known for the present time.
- Accuracy degrades for times further in the past.

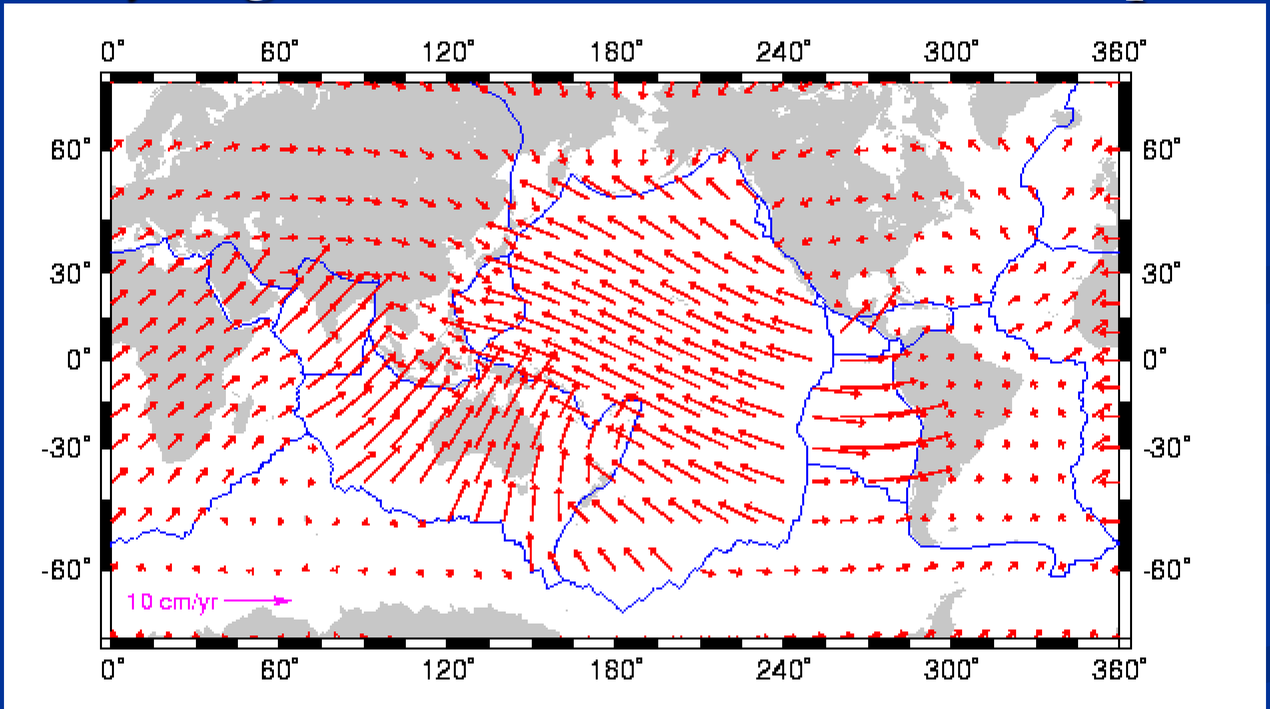

Data: Argus & Gordon 1991 (NUVEL-NNR), Figure: T. Becker

Plate Motion

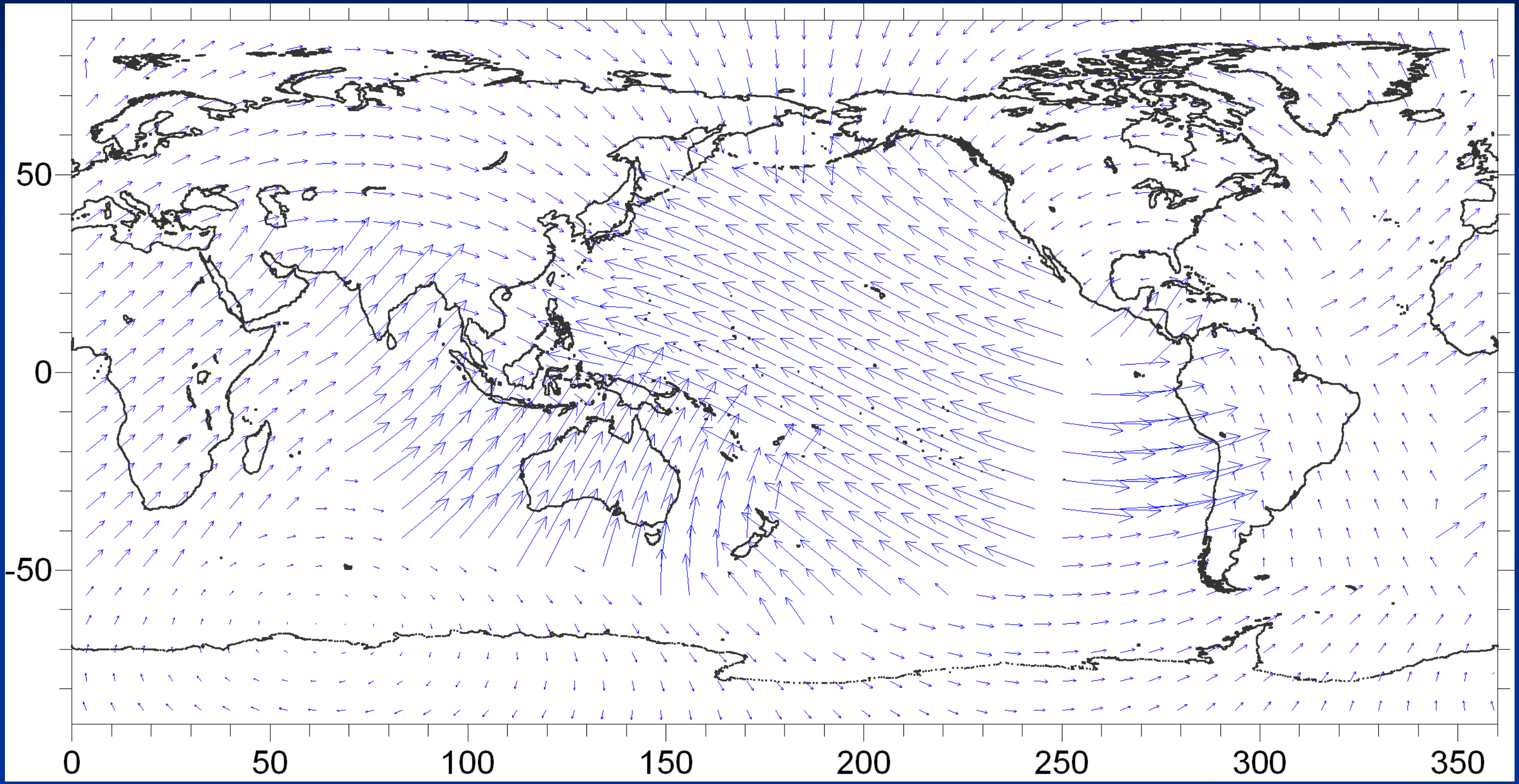

Observed plate velocities in no-net-rotation (NNR) reference frame

Plate Motion

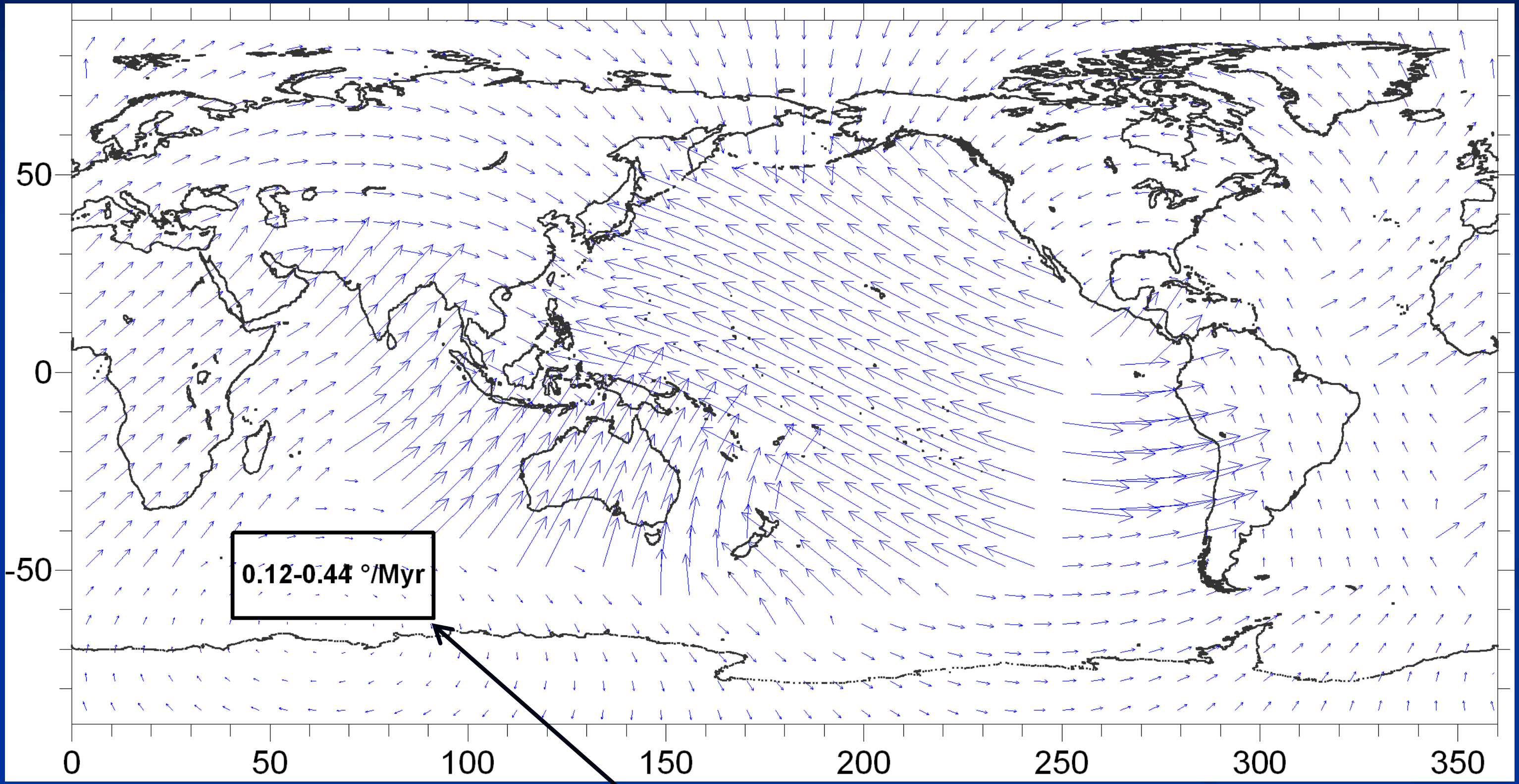

… and observed net-rotation (NR) of the lithosphere

Based on analyses of seismic anisotropy Becker (2008) narrowed possible range of angular NR velocities down to **0.12-0.22 °/Myr**

Seismic Tomography

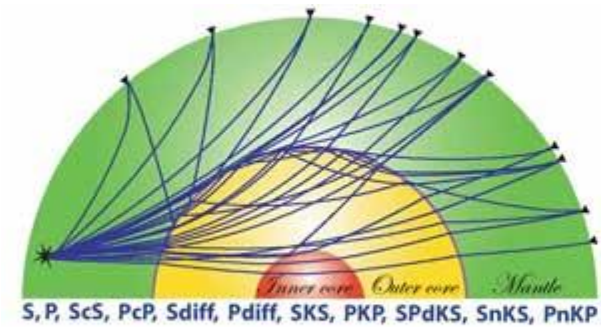

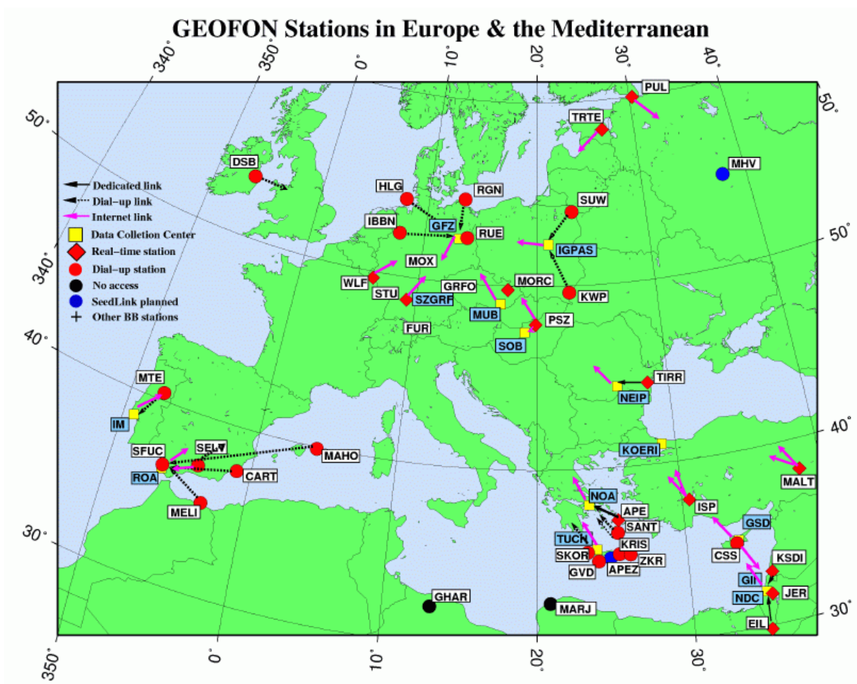

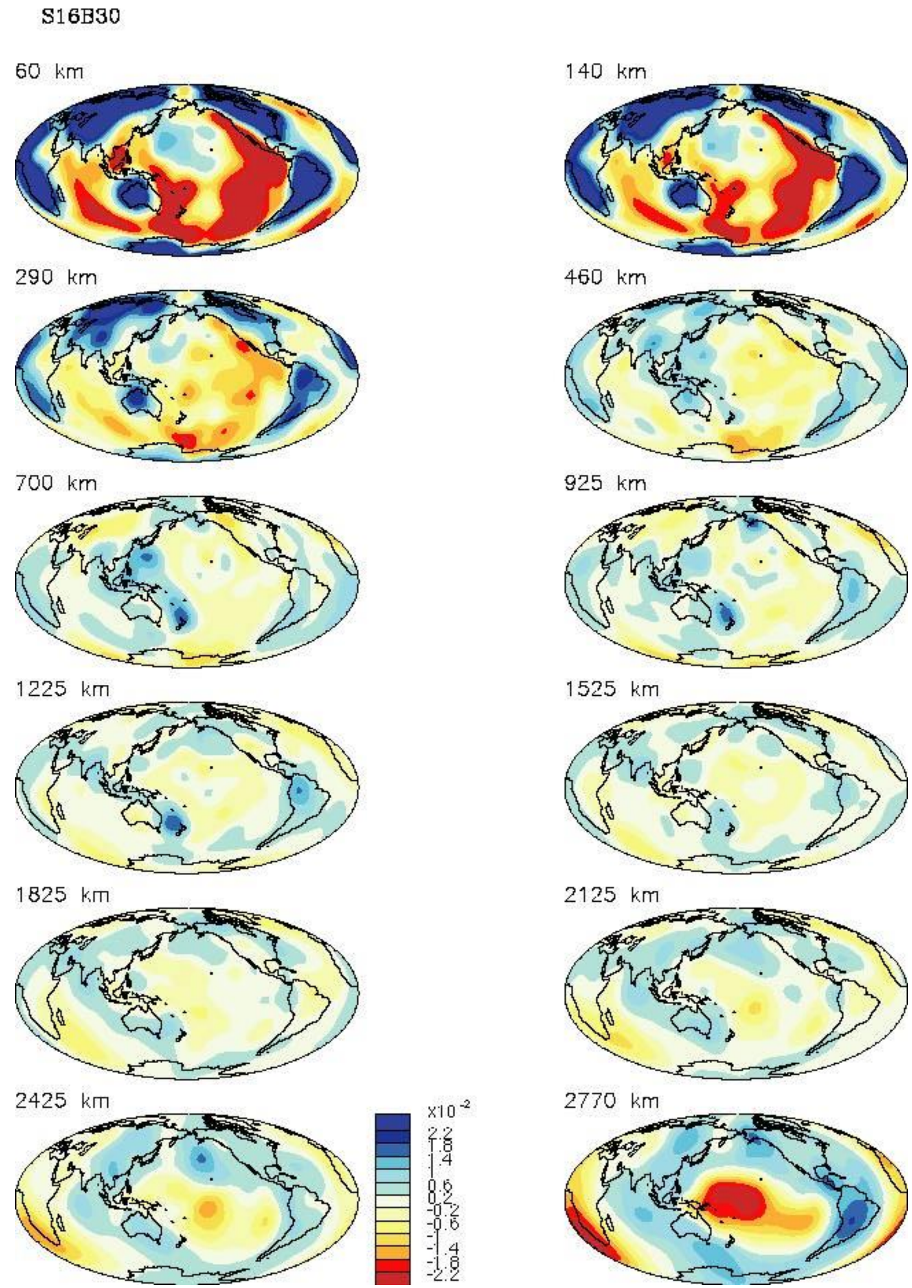

Summary of Surface Observations

Observation	Quality .
Plate Motion	good (recent)
Geoid	good (<100 km)
Free-air Gravity	good (shallow)
Dynamic Topography	poor (magnitude)
Post Glacial Rebound	variable (center)

Seismic Tomography	best to constrain deep structure

Stokes equations

$$\frac{\partial v_i}{\partial x_i} = 0$$

$$-\frac{\partial P}{\partial x_i} + \frac{\partial}{\partial x_j}(\eta(\frac{\partial v_i}{\partial x_j} + \frac{\partial v_j}{\partial x_i})) + \rho(x_1, x_2, x_3) g_i = 0$$

Main tool to model mantle convection

Solution is most simple if viscosity depends only on depth

$$v_i = \sum_{l=0}^{\infty} \sum_{m=-l}^{l} V_{lm}^{i}(r) Y_{lm}(\varphi, \vartheta)$$

$$P = \int \rho g dr + \sum_{l=0}^{\infty} \sum_{m=-l}^{l} P_{lm}(r) Y_{lm}(\varphi, \vartheta)$$

Stokes equations

$$\frac{\partial v_i}{\partial x_i} = 0$$

$$-\frac{\partial P}{\partial x_i} + \frac{\partial}{\partial x_j}\left(\eta\left(\frac{\partial v_i}{\partial x_j} + \frac{\partial v_j}{\partial x_i}\right)\right) + \boxed{\rho(x_1, x_2, x_3)}\, g_i = 0$$

Main tool to model mantle convection

Solution is most simple if viscosity depends only on depth

$$v_i = \sum_{l=0}^{\infty} \sum_{m=-l}^{l} V_{lm}^{i}(r) Y_{lm}(\varphi, \vartheta)$$

$$P = \int \rho g dr + \sum_{l=0}^{\infty} \sum_{m=-l}^{l} P_{lm}(r) Y_{lm}(\varphi, \vartheta)$$

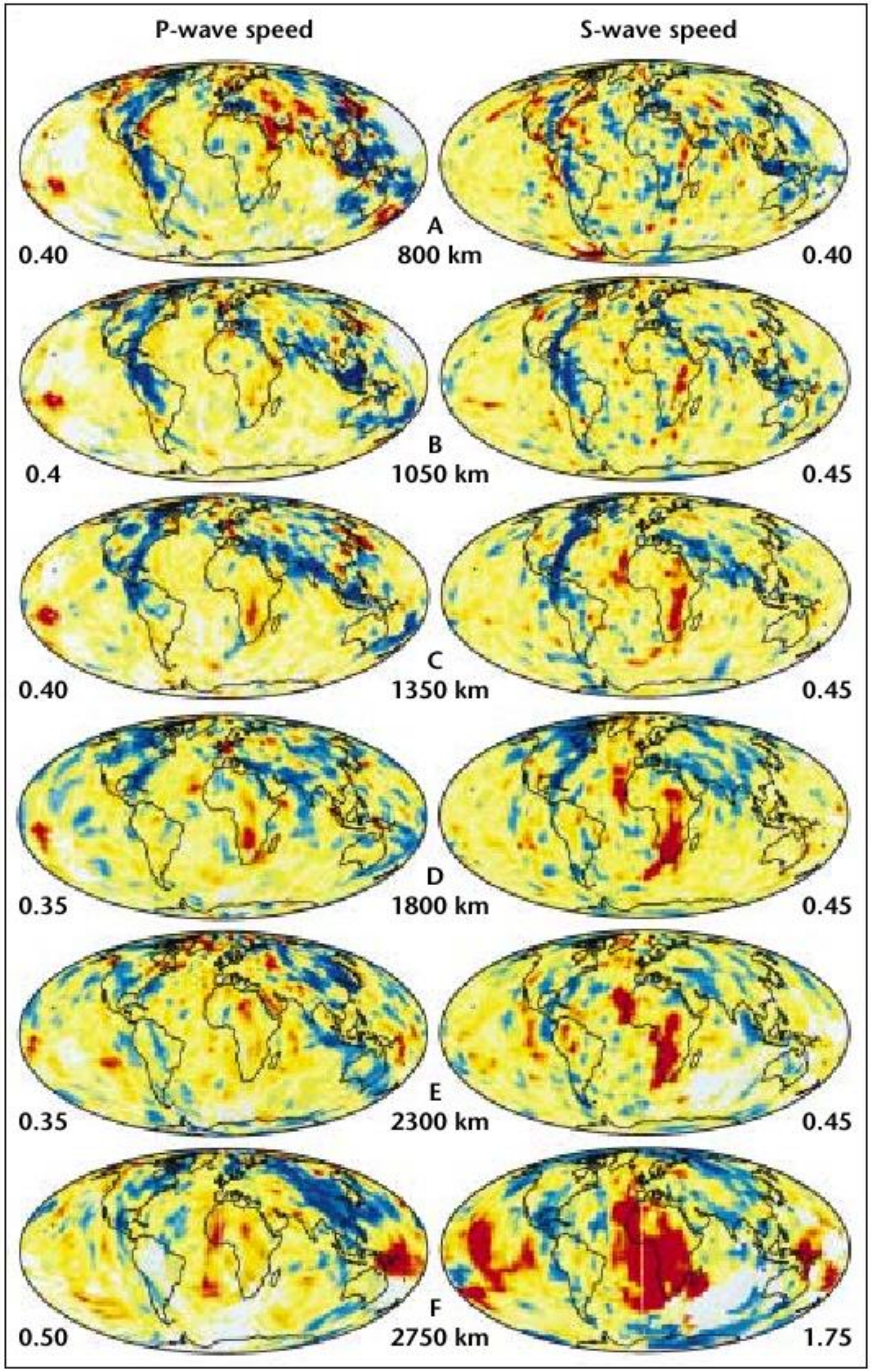

Left: Tomography (Grand et al. 1997)

Right: Subduction history

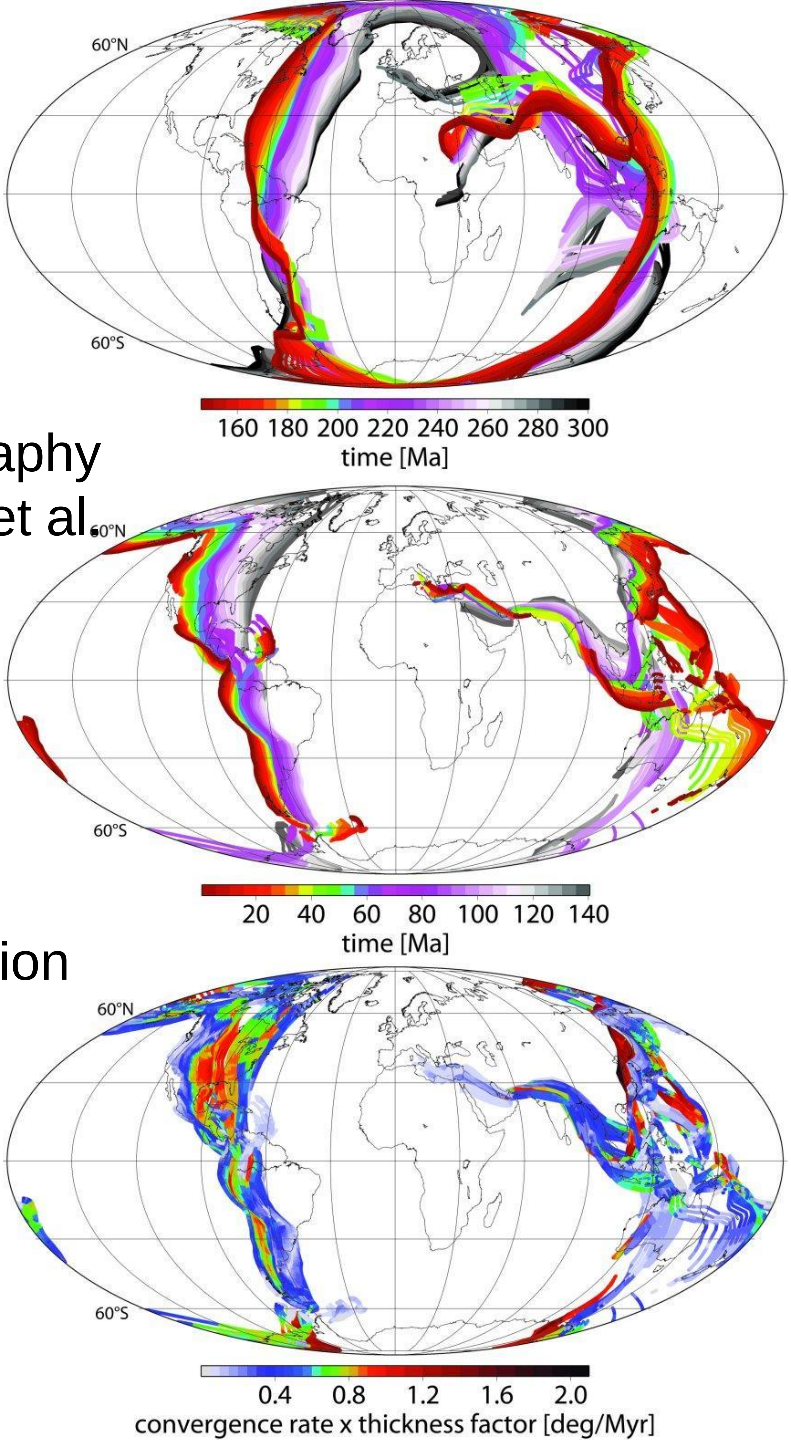

Stokes equations (thermal convection)

$$\cancel{\alpha \frac{DT}{Dt}} + \frac{\partial v_i}{\partial x_i} = 0$$

$$-\frac{\partial P}{\partial x_i} + \frac{\partial}{\partial x_j}\left(\eta\left(\frac{\partial v_i}{\partial x_j} + \frac{\partial v_j}{\partial x_i}\right)\right) = \rho_0 (1 - \alpha (T - T_0)) g_i$$

Boussinesq approximation

$$\rho C_p \frac{DT}{Dt} = \frac{\partial}{\partial x_i}\left(\lambda \frac{\partial T}{\partial x_i}\right) + \cancel{\frac{1}{\eta_{eff}}\tau_{ij}\tau_{ij}} + \rho A + \cancel{\Delta H_{chem}}$$

$$P = \rho_0 g x_3 + \Delta P \qquad Ra = \frac{\alpha_0 g_0 \rho_0 H^3 \Delta T}{k_0 \eta_0}$$ Rayleigh number

A Simple Picture of the Mantle: Boundary Layers

Montelli et al. [2004]

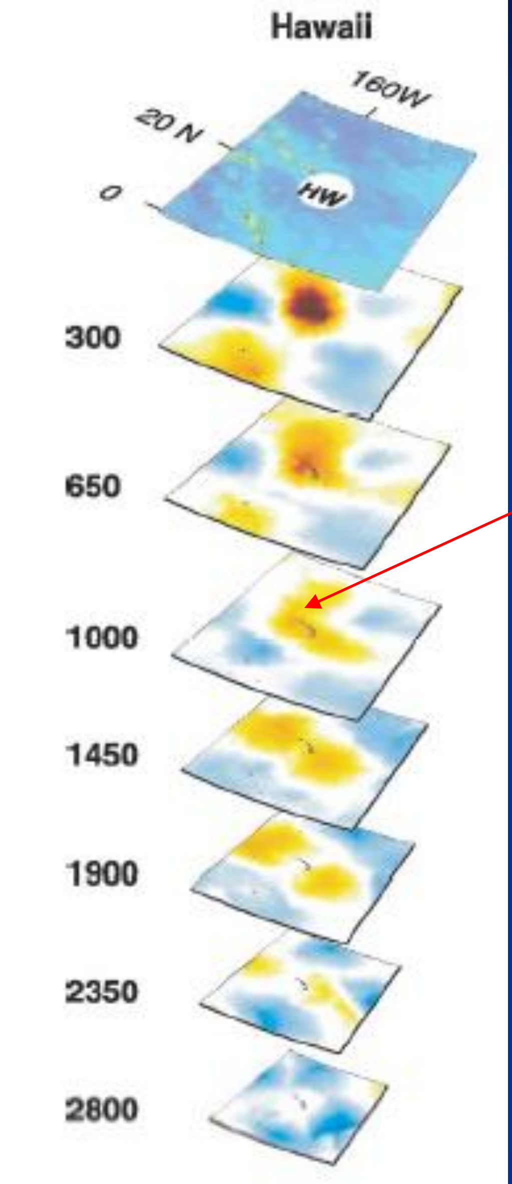

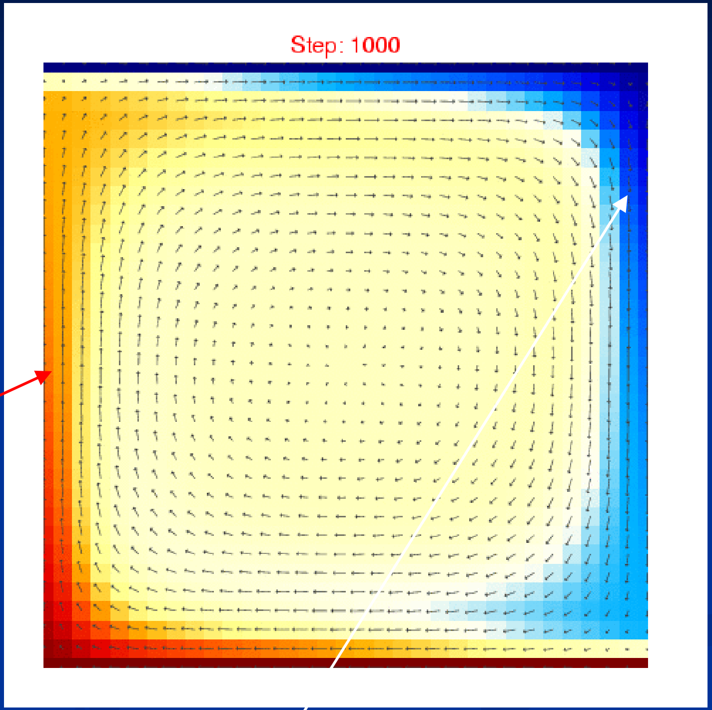

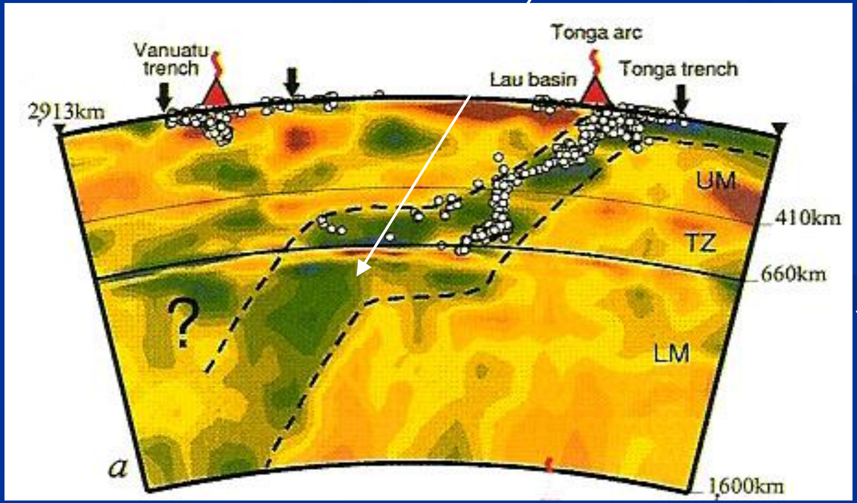

van der Hilst [1995]

Mantle convection typical 2D model

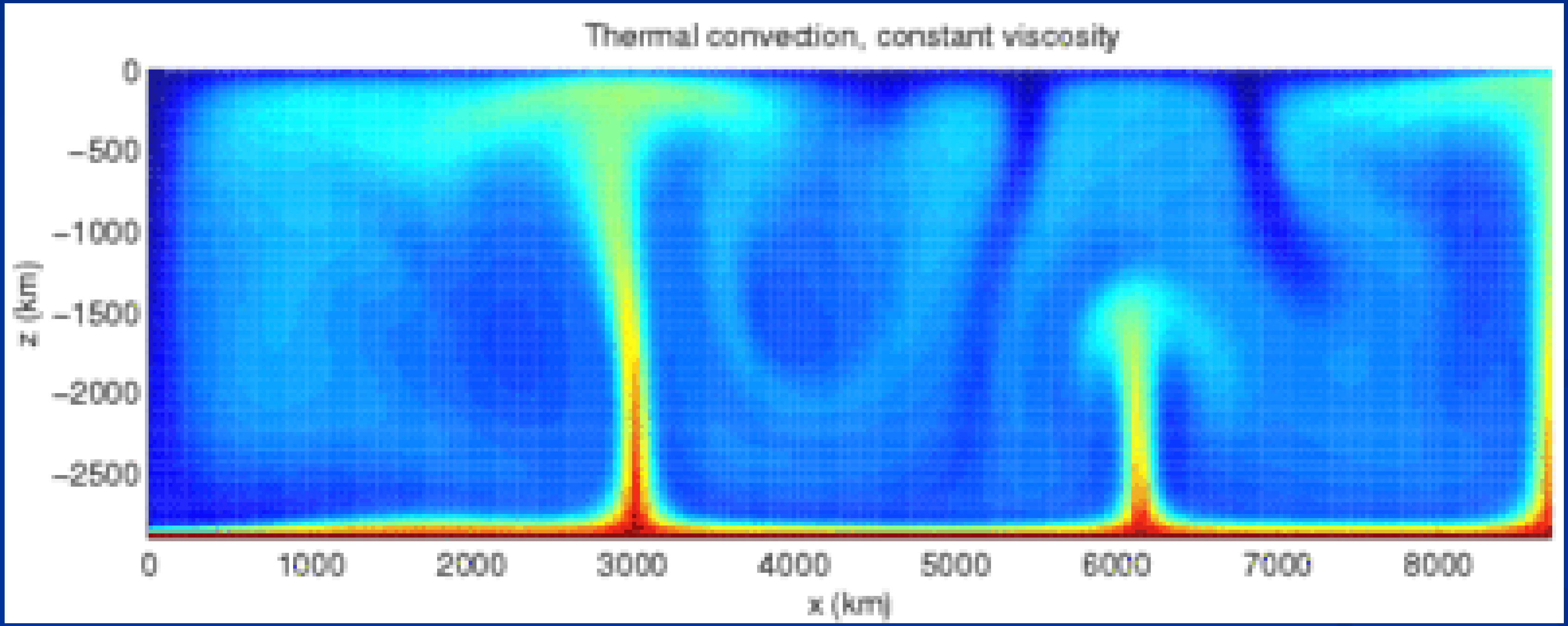

Two separated geochemical reservoirs in the mantle

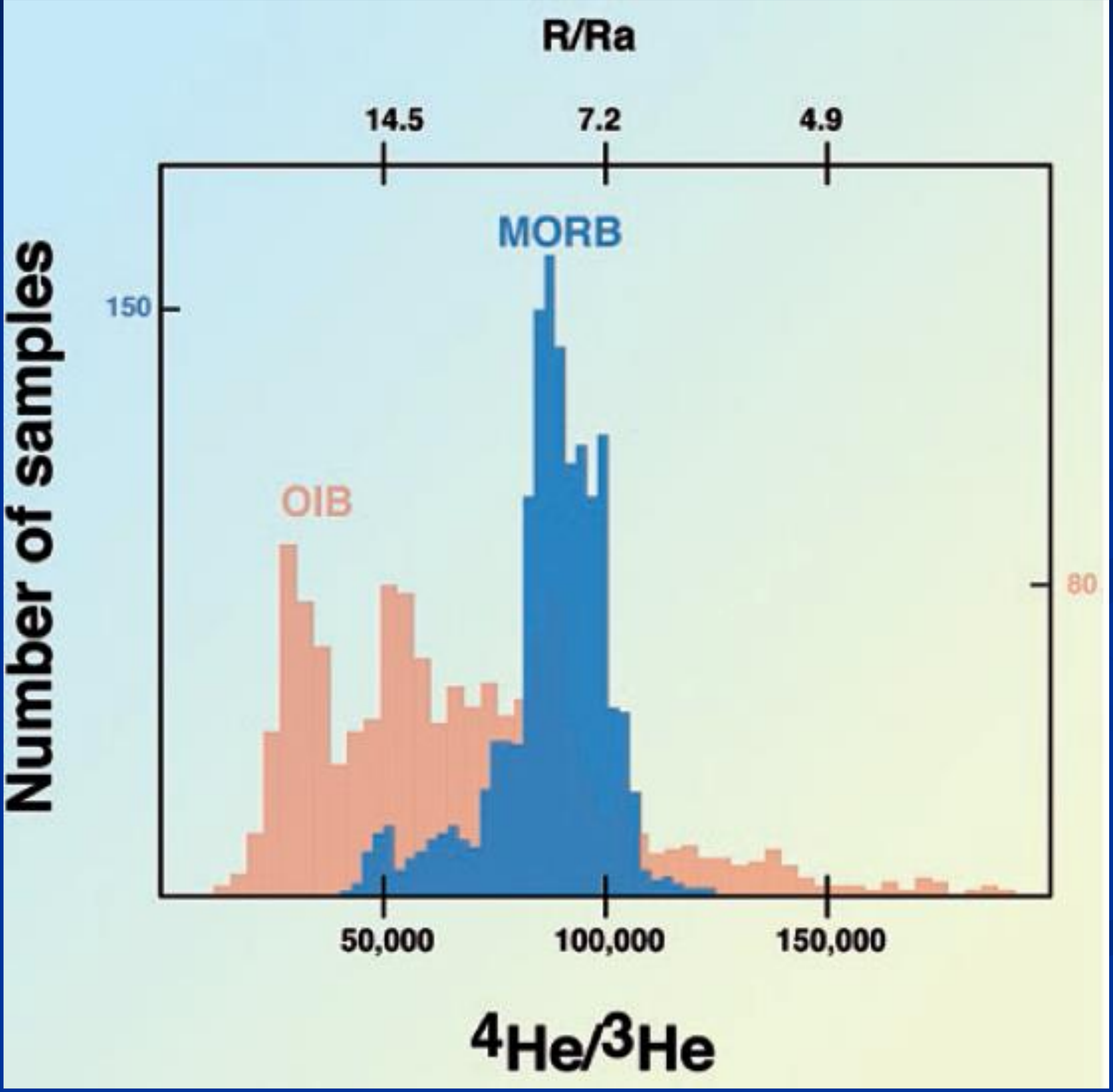

Mantle convection geochemical picture

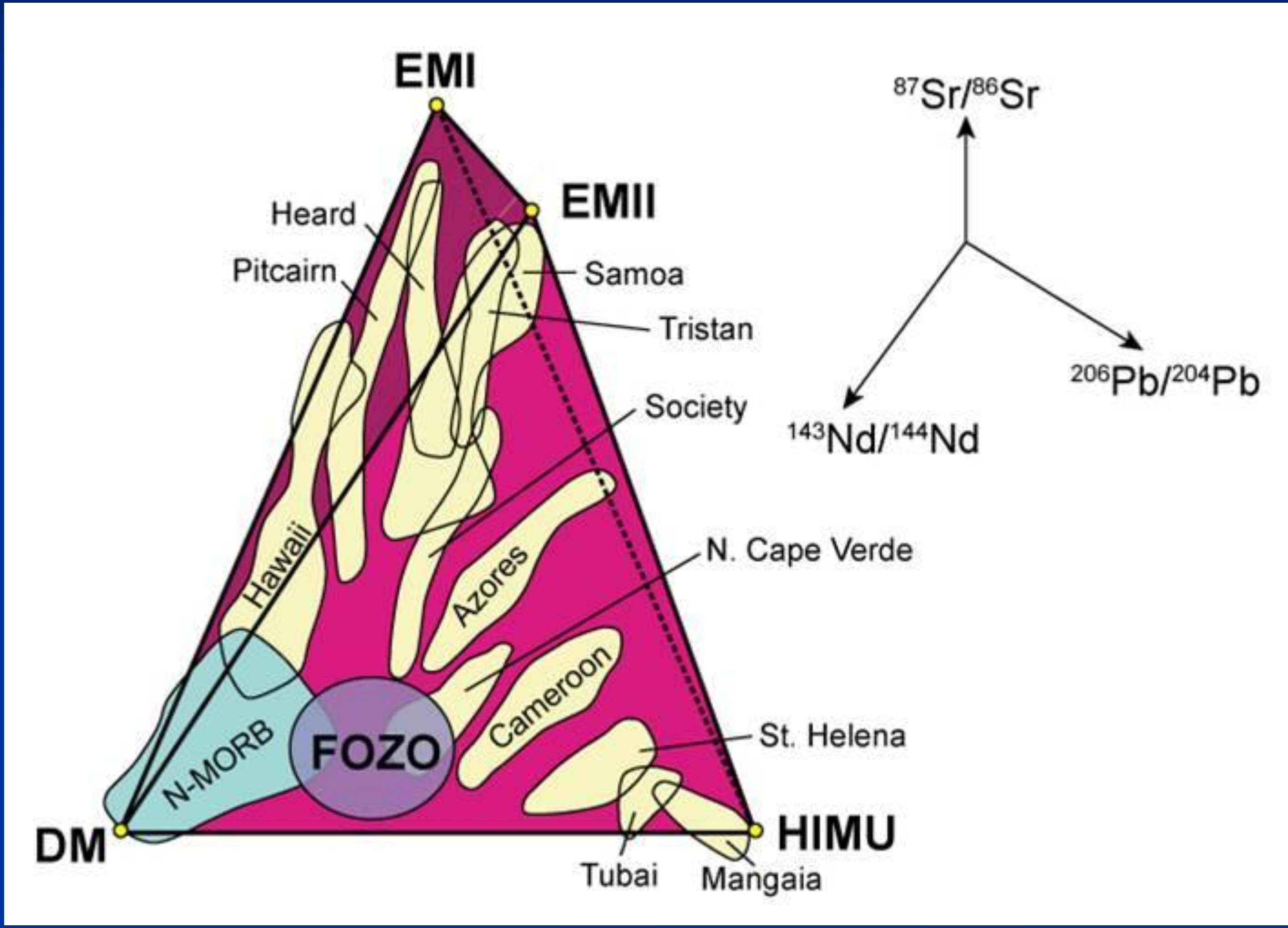

Mantle convection geochemical picture

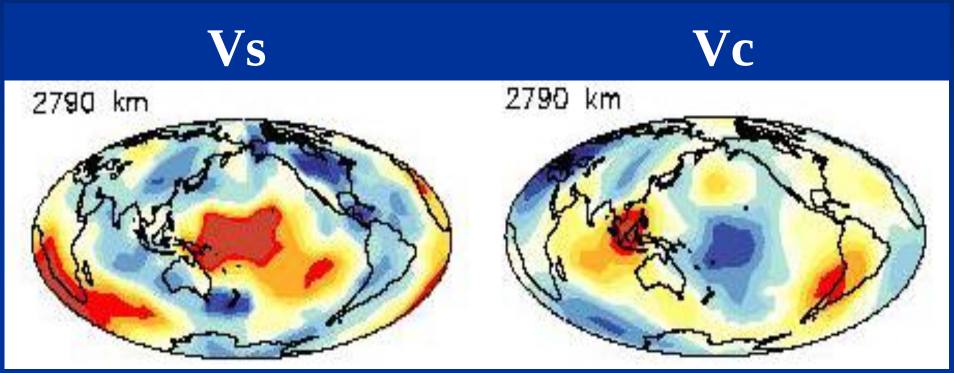

Masters et al. [2000]. Ishii & Trump [1999]

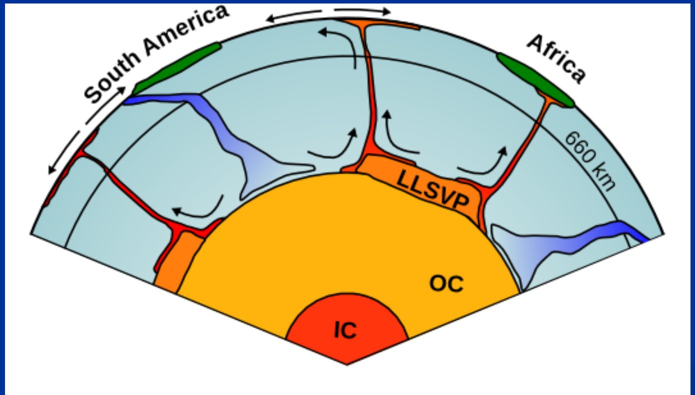

Figure 1: Limitation of plume generation zones by subducting slabs and thermo-chemical piles.

Seismic tomography supports whole-mantle convection

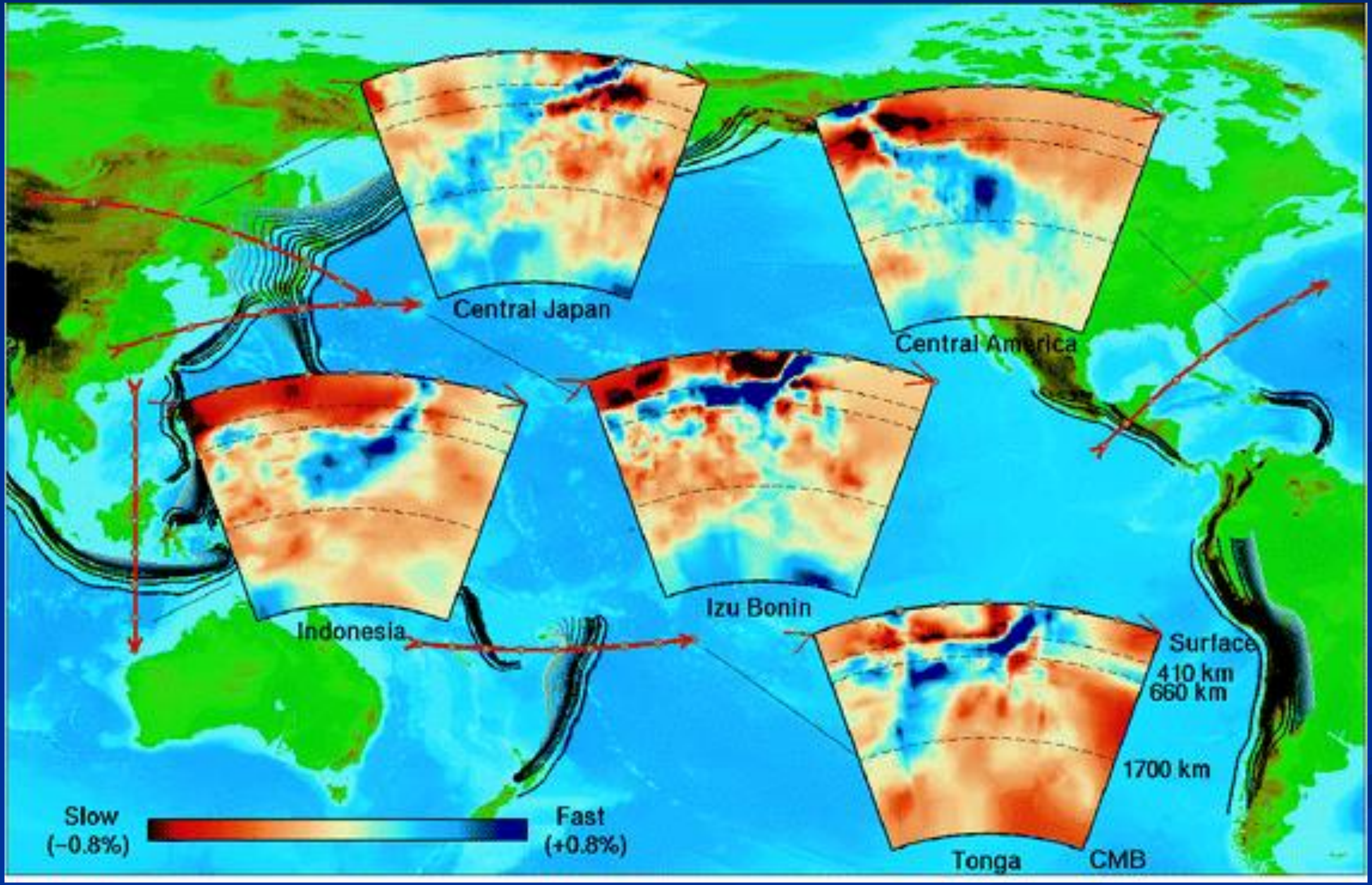

(From Stern, R.J., Subduction Zones, Rev. Geophys. 2002)

What kind of tectonics should be expected with "normal" mantle convection?

$$\eta \approx exp(H_a/nRT)$$

Stagnant-lid tectonics→ convection beneath the outer shall (lid) and no much deformation near the surface

Solving Stokes equations with FE code Terra

(Bunge et al.)

Mantle convection

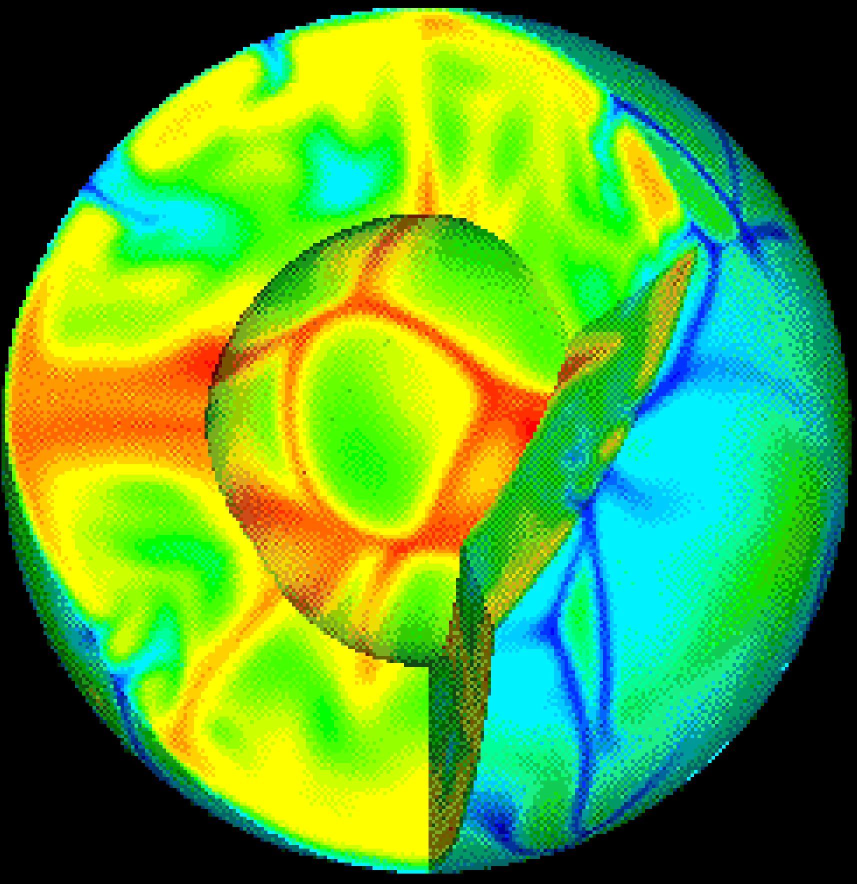

$$\eta = \min(\eta(P,T), \eta_{\max})$$

$$\eta = \min(\eta(P,T), \frac{\sigma_Y}{\dot{\varepsilon}_{II}})$$

Ingredients of plate tectonics

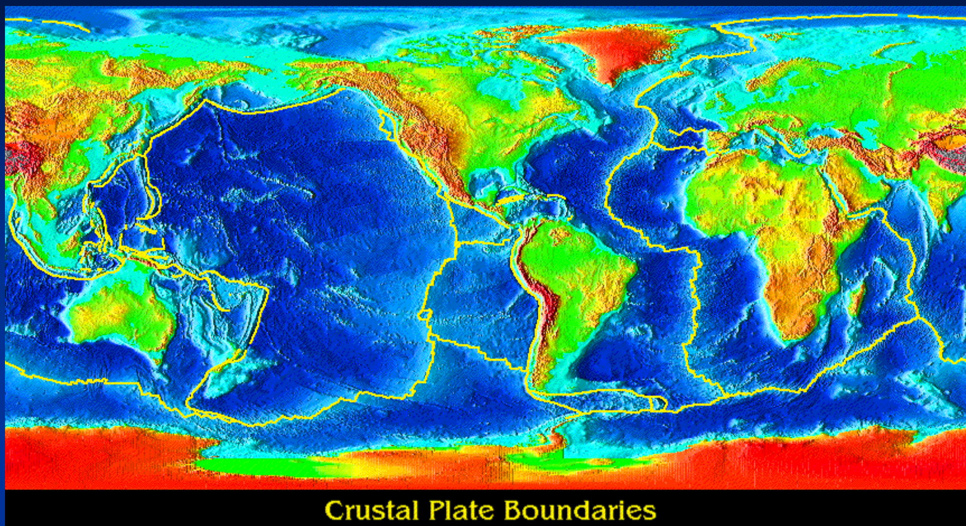

Convection (FE code Terra)

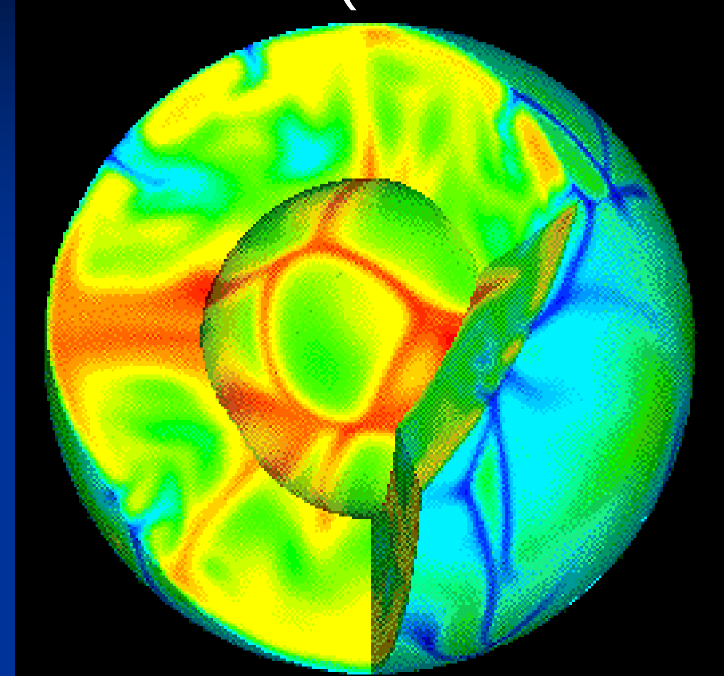

Weak plate boundaries

Ricard and Vigny, 1989; Bercovici, 1993; Bird, 1998; Moresi and Solomatov, 1998;Tackley, 1998, Zhong et al, 1998; Trompert and Hansen, 1998;Gurnis et al., 2000….

Thermal Convection with Temperature-dependent Viscosity and Plates

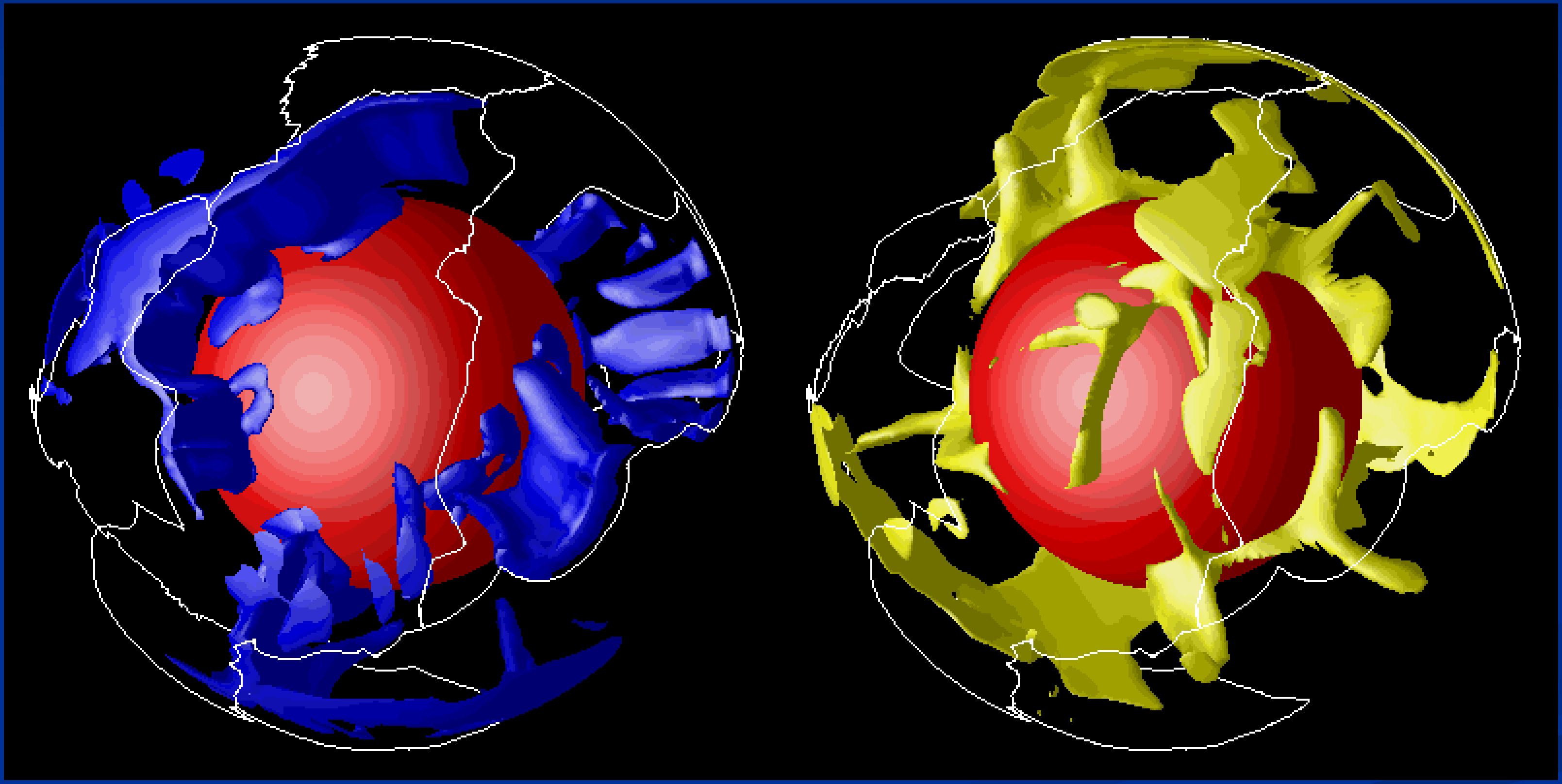

Zhong, Zuber, Moresi, & Gurnis [2000]

Ingredients of plate tectonics

Increasing yield stress

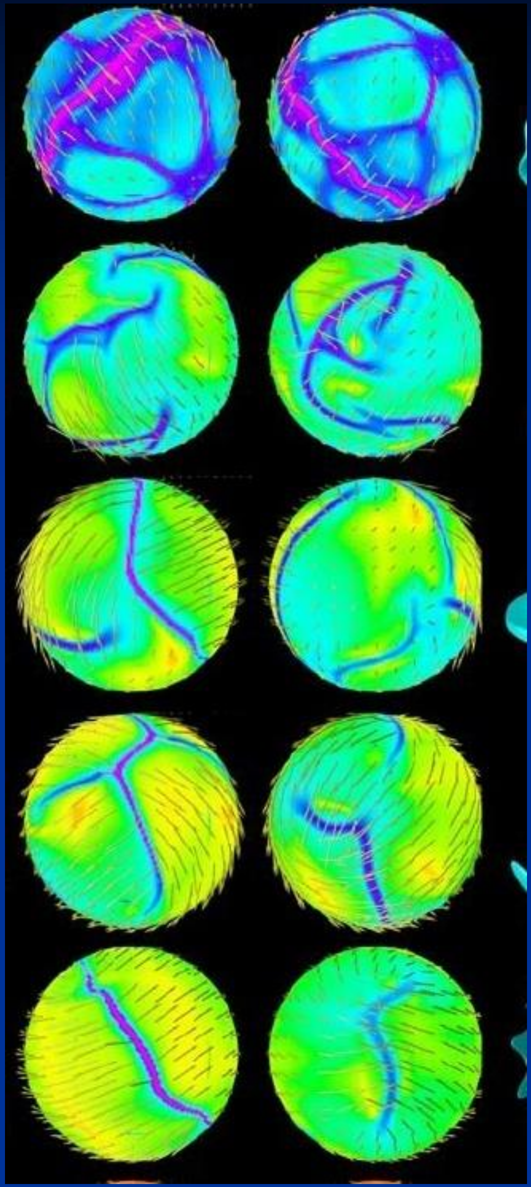

van Heck and Tackley, 2008

Generating plate boundaries

Bercovici, 1993,1995, 1996, 1998, 2003; Tackley, 1998, 2000; Moresi and Solomatov, 1998; Zhong et al, 1998; Gurnis et al., 2000…

Tendency: towards more realistic strongly non-linear rheology

Viscous rheology-only and emulation of brittle failure

Solving Stokes equations with code Rhea

(adaptive mesh refinement)

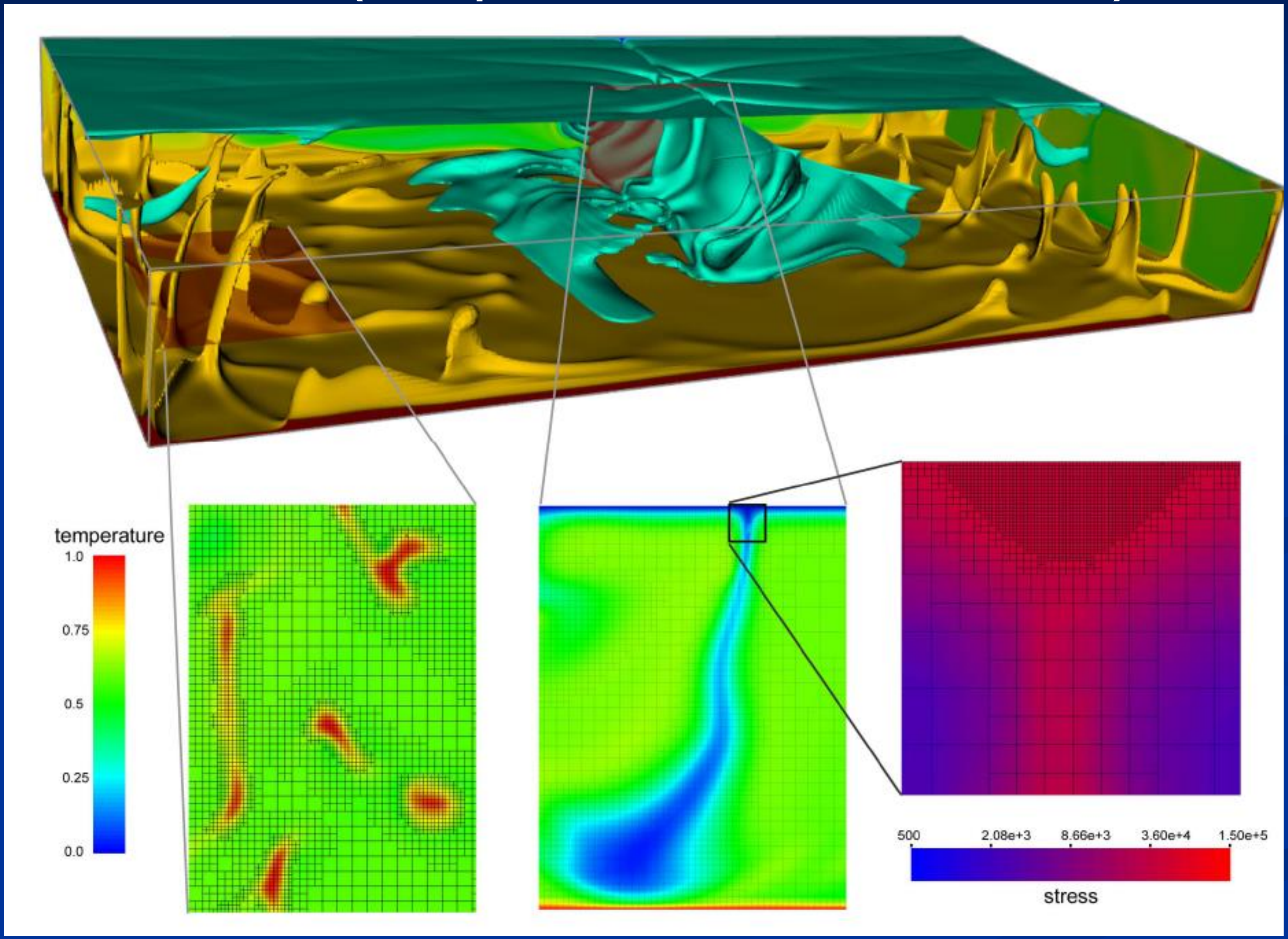

Burstedde et al.,2008-2010

Solving Stokes equations with code Rhea

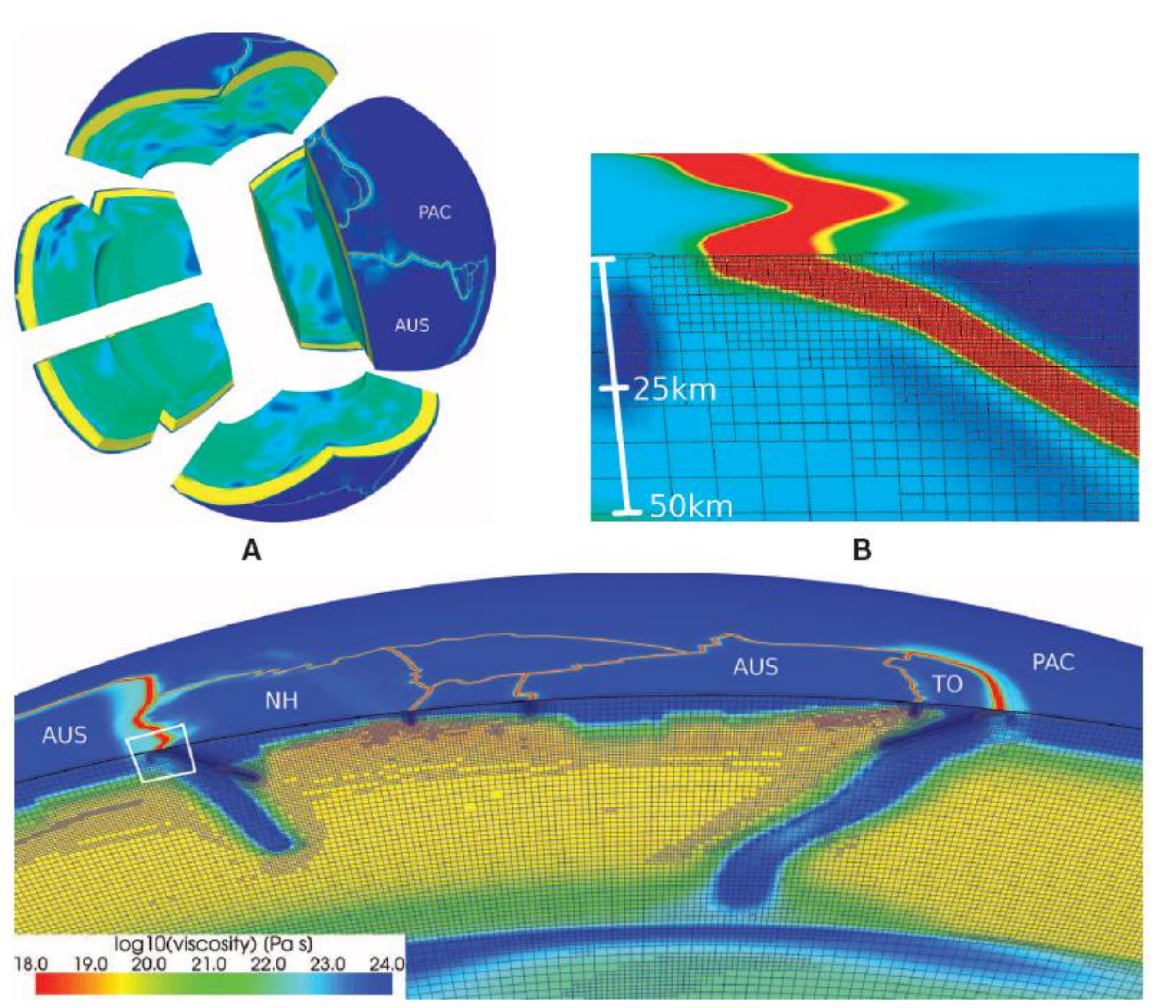

Stadler et al., 2010

Point 1

Global models can not generate yet present-day plates and correctly reproduce plate motions

They employ plastic (brittle) rheolgical models inconsistent with laboratory data

They have difficulty to reproduce realistic one-sided subduction and pure transform boundaries

Modeling deformation at plate boundaries

Subduction and orogeny in Andes

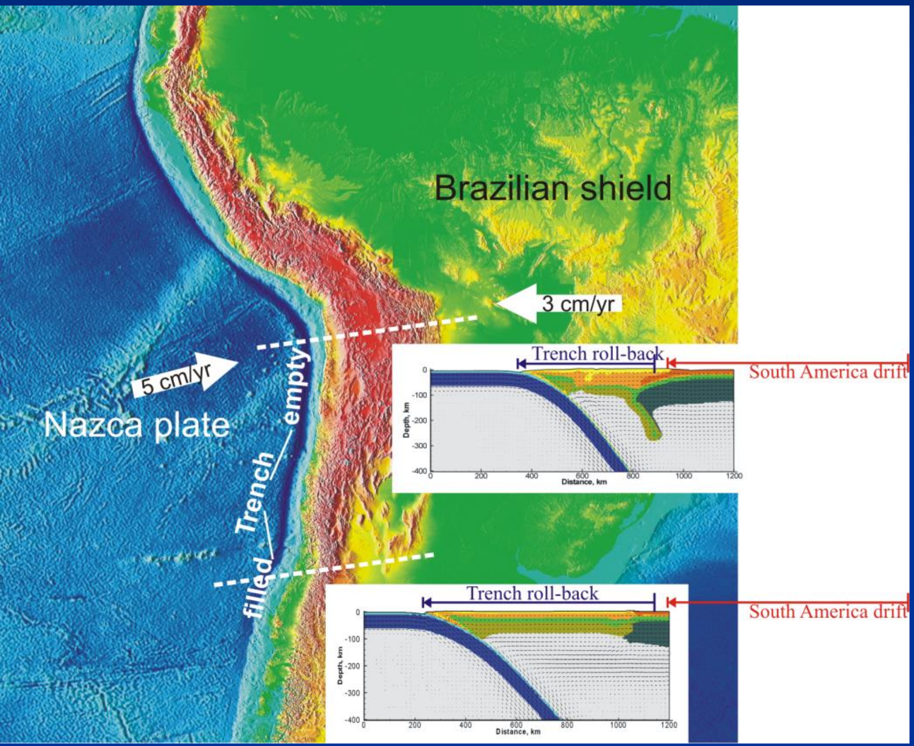

Sobolev and Babeyko, *Geology* 2005; Sobolev et al., 2006

Dead Sea Transform

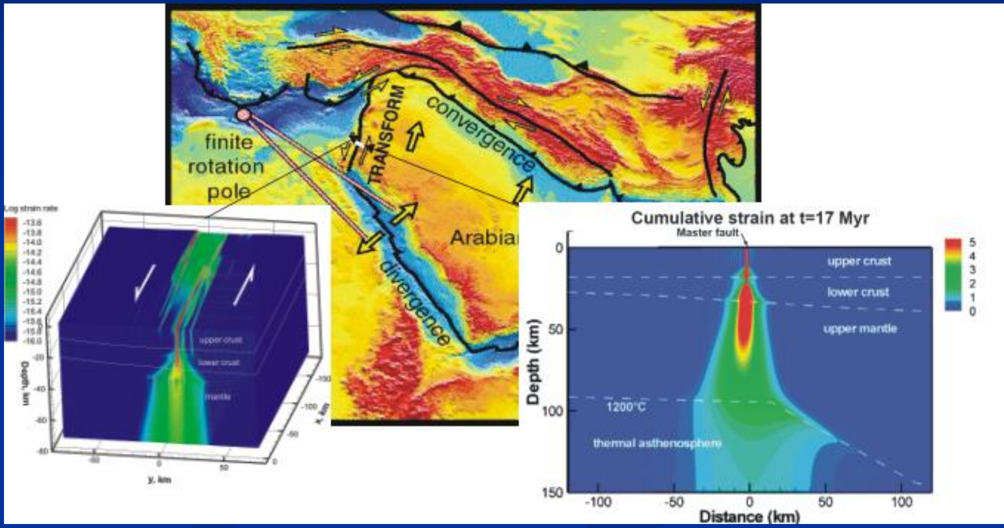

(Sobolev et al., *EPSL* 2005, Petrunin and Sobolev, *Geology* 2006, *PEPI*, 2008).

„Realistic“ rheology

Balance equations

Momentum: $$\frac{\partial \sigma_{ij}}{\partial x_j} + \Delta\rho g\, z_i = 0$$

Energy: $$\frac{DU}{Dt} = -\frac{\partial q_i}{\partial x_i} + r$$

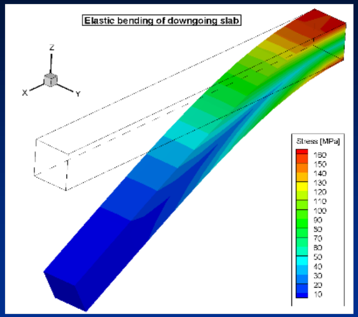

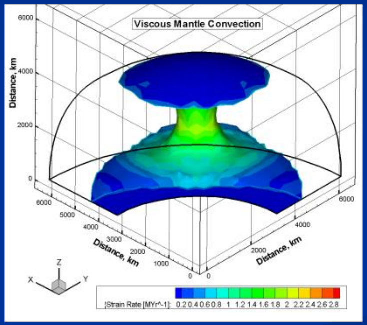

Deformation mechanisms

$$\dot{\varepsilon}_{ij} = \dot{\varepsilon}_{ij}^{el} + \dot{\varepsilon}_{ij}^{vs} + \dot{\varepsilon}_{ij}^{pl}$$

Elastic strain: $$\dot{\varepsilon}_{ij}^{el} = \frac{1}{2G}\hat{\tau}_{ij}$$

Viscous strain: $$\dot{\varepsilon}_{ij}^{vs} = \frac{1}{2\eta_{eff}}\tau_{ij}$$

Plastic strain: $$\dot{\varepsilon}_{ij}^{pl} = \dot{\gamma}\frac{\partial Q}{\partial \tau_{ij}}$$

Mohr-Coulomb

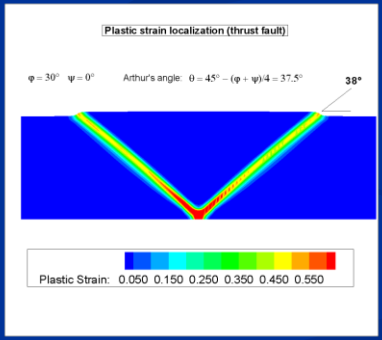

Popov and Sobolev (PEPI, 2008)

Three creep processes

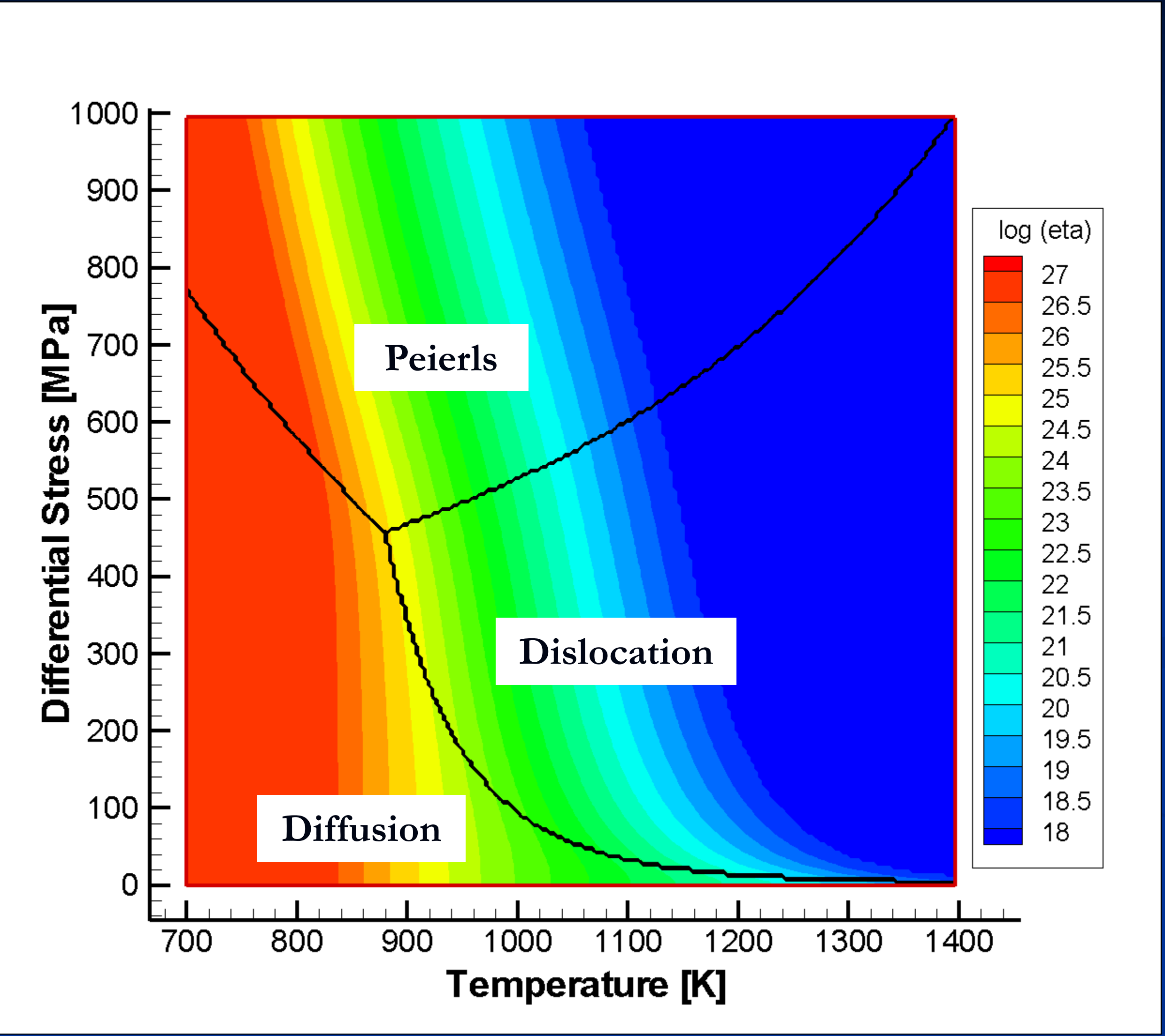

$$\eta_{eff} = \tfrac{1}{2}\tau_{II}\left(\dot{\varepsilon}_L + \dot{\varepsilon}_N + \dot{\varepsilon}_P\right)^{-1}$$

Diffusion creep

$$\dot{\varepsilon}_L = B_L \tau_{II} \exp\left(-\frac{E_L}{RT}\right)$$

Dislocation creep

$$\dot{\varepsilon}_N = B_N \left(\tau_{II}\right)^n \exp\left(-\frac{E_N}{RT}\right)$$

Peierls creep

$$\dot{\varepsilon}_P = B_P \exp\left[-\frac{E_P}{RT}\left(1 - \frac{\tau_{II}}{\tau_P}\right)^2\right]$$

(Kameyama *et al.* 1999)

Combining global and lithospheric-scale models

Coupling mantle convection and lithospheric deformation

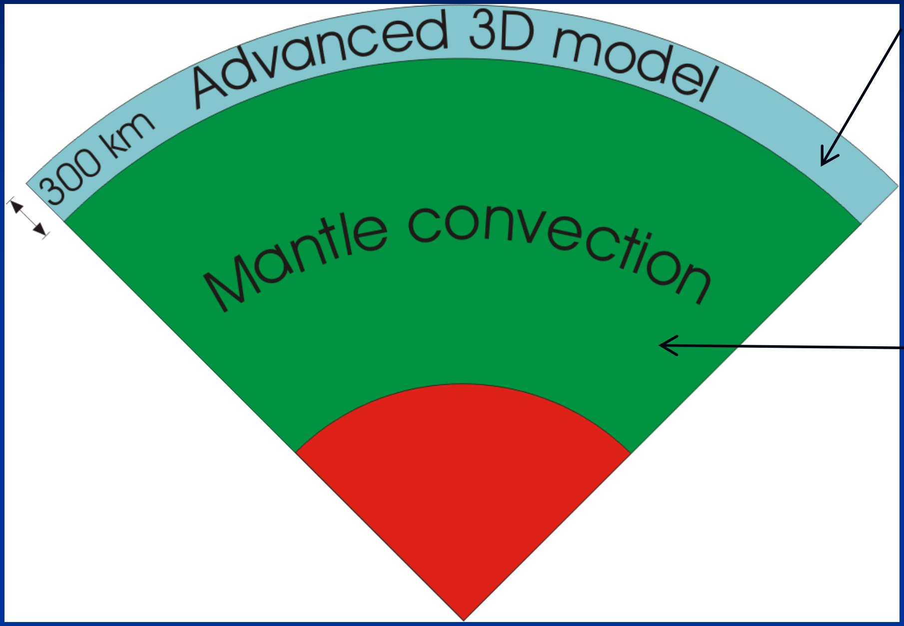

Lithospheric code (Finite Elements)

Mantle code (spectral or FEM)

Mantle and lithospheric codes are coupled through continuity of velocities and tractions at 300 km.

Sobolev, Popov and Steinberger, in preparation

Above 300 km depth

3D temperature from surface heat flow at continents and ocean ages in oceans, crustal structure from model crust2.0

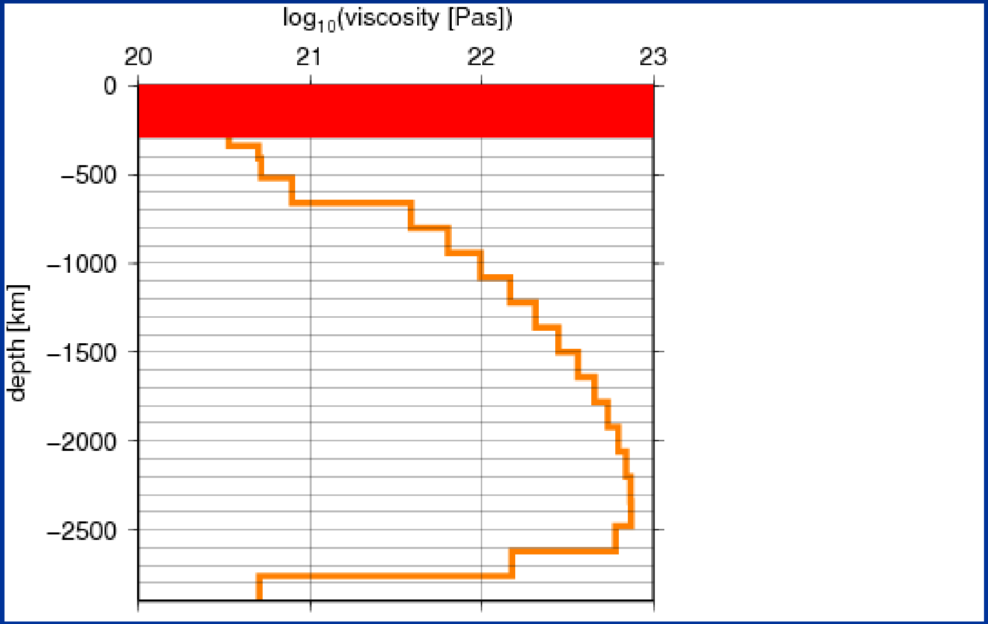

Below 300 km depth

Spectral method (Hager and O'Connell,1981) with radial viscosity and **3D density distributions** based on subduction history (Steinberger, 2000)

Mantle rheology

olivine rheology with water content as model parameter

$$\dot{\varepsilon}_{II} = A d^{-m} C_{H2O}^{p} \sigma_{II}^{n} \exp(-(E_a + PV_a)/RT)$$

Parameters in reference model from laboratory data by Hirth and Kohlstedt (2003) with **n=3.5 +-0.3**.

Plate boundaries

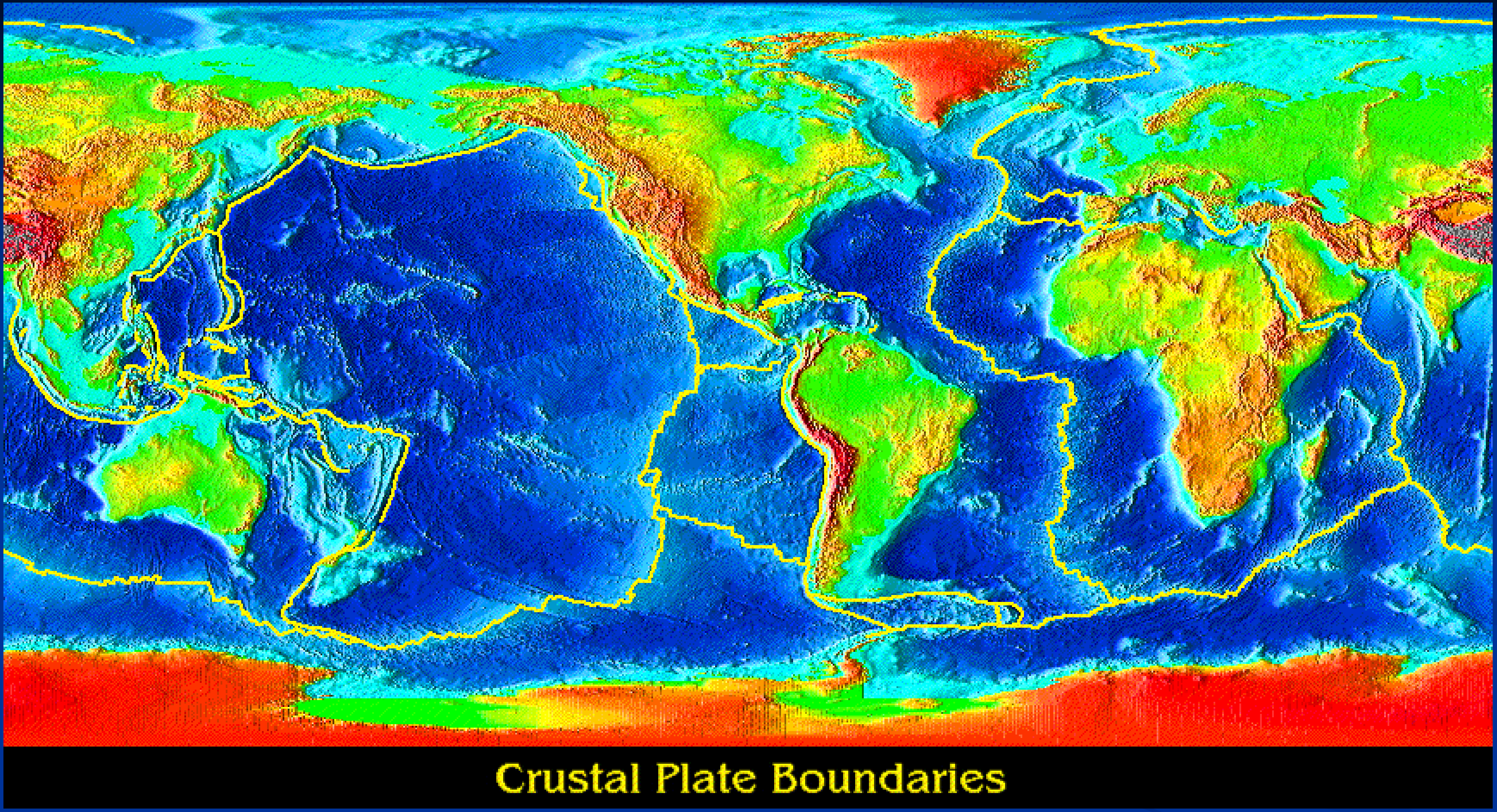

Plate boundaries are defined as narrow zones with visco-plastic rheology where friction coefficient is model parameter

Lithospheric code (FEM)

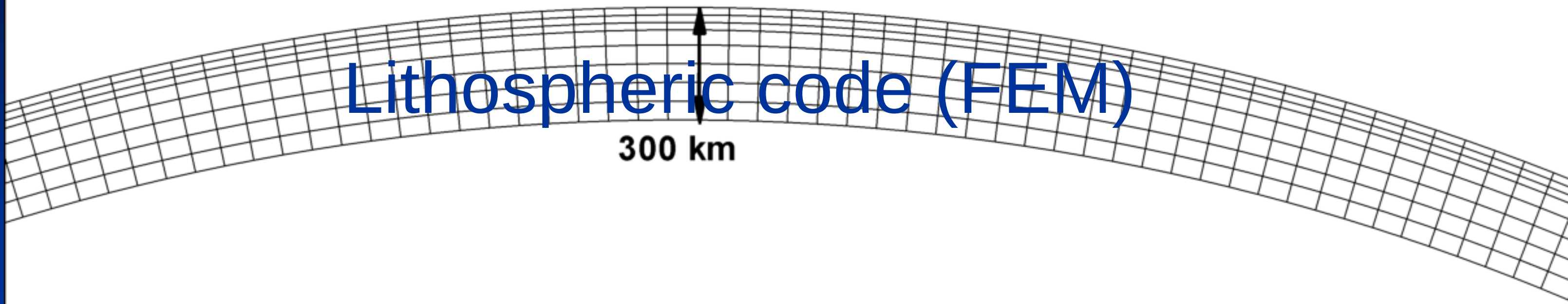

Mantle code (spectral)

Mantle and lithospheric codes are coupled through continuity of velocities and tractions at 300 km.

The model has **free surface** and **3D**, strongly **non-linear visco-elastic rheolog**y with **true plasticity** (brittle failure) in upper 300km.

Mesh for low-resolution model

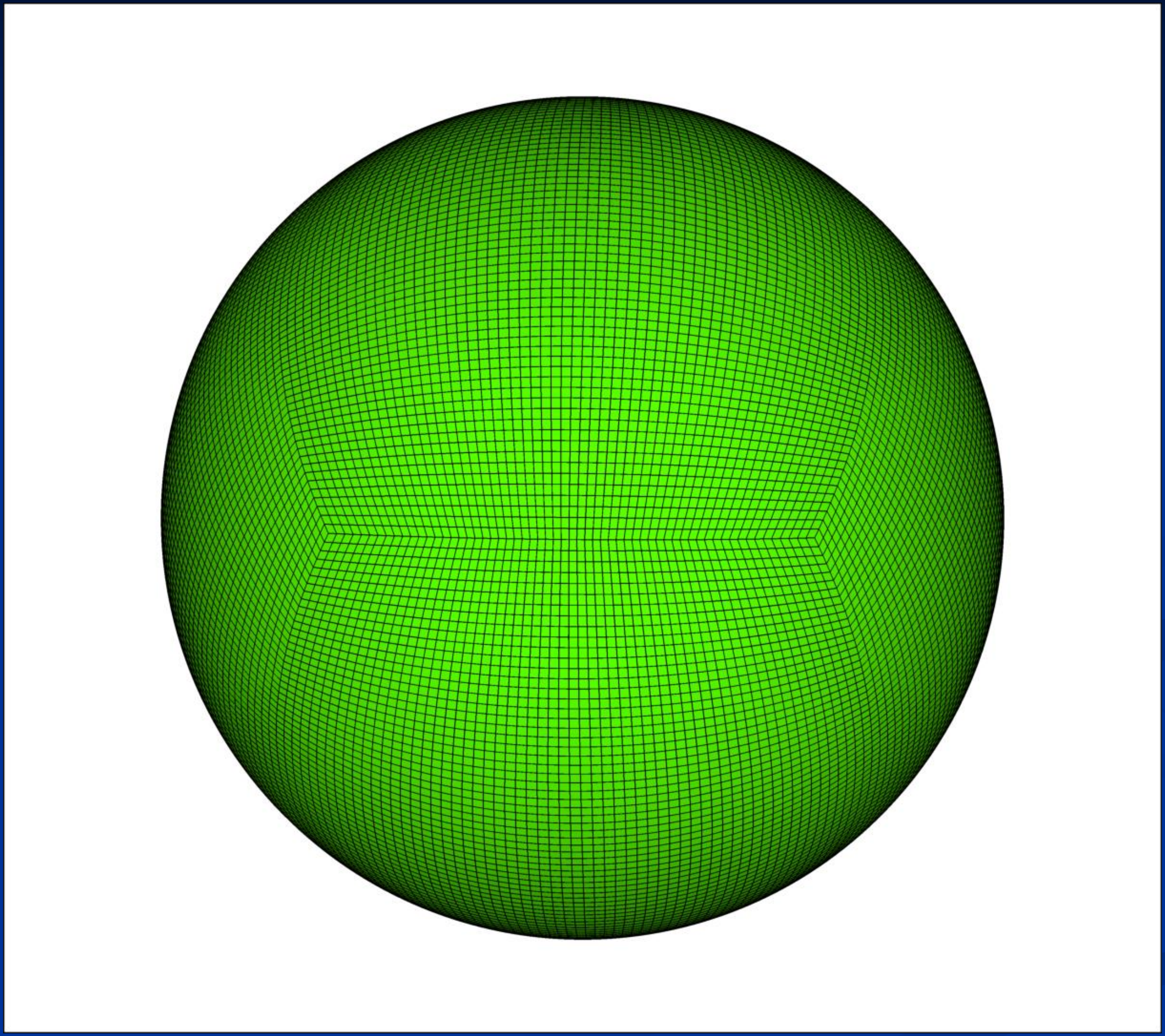

How weak are plate boundaries?

Effect of strength at plate boundaries

Friction at boundaries 0.4 (Smax=600 MPa)

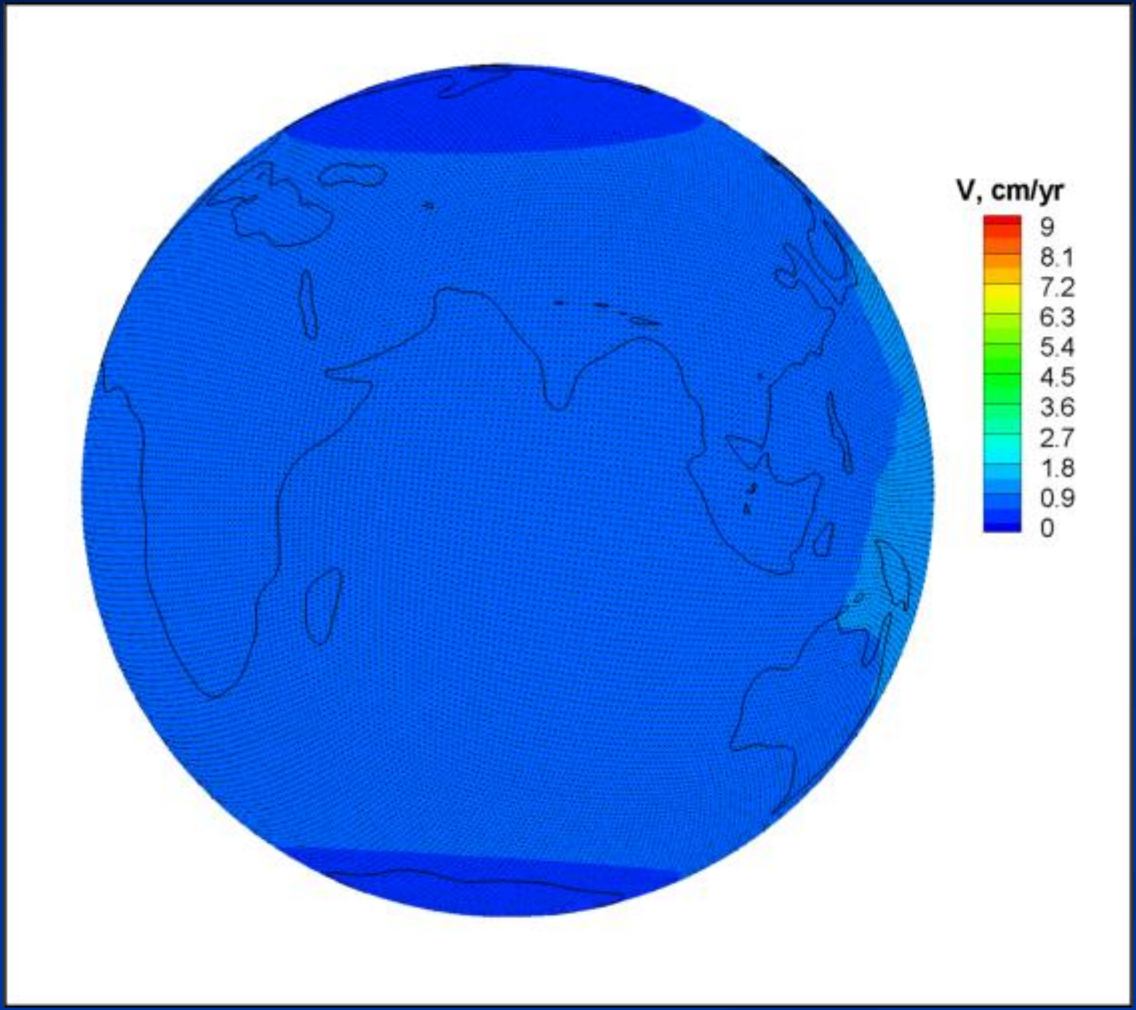

Friction at boundaries 0.2 (Smax=300 MPa)

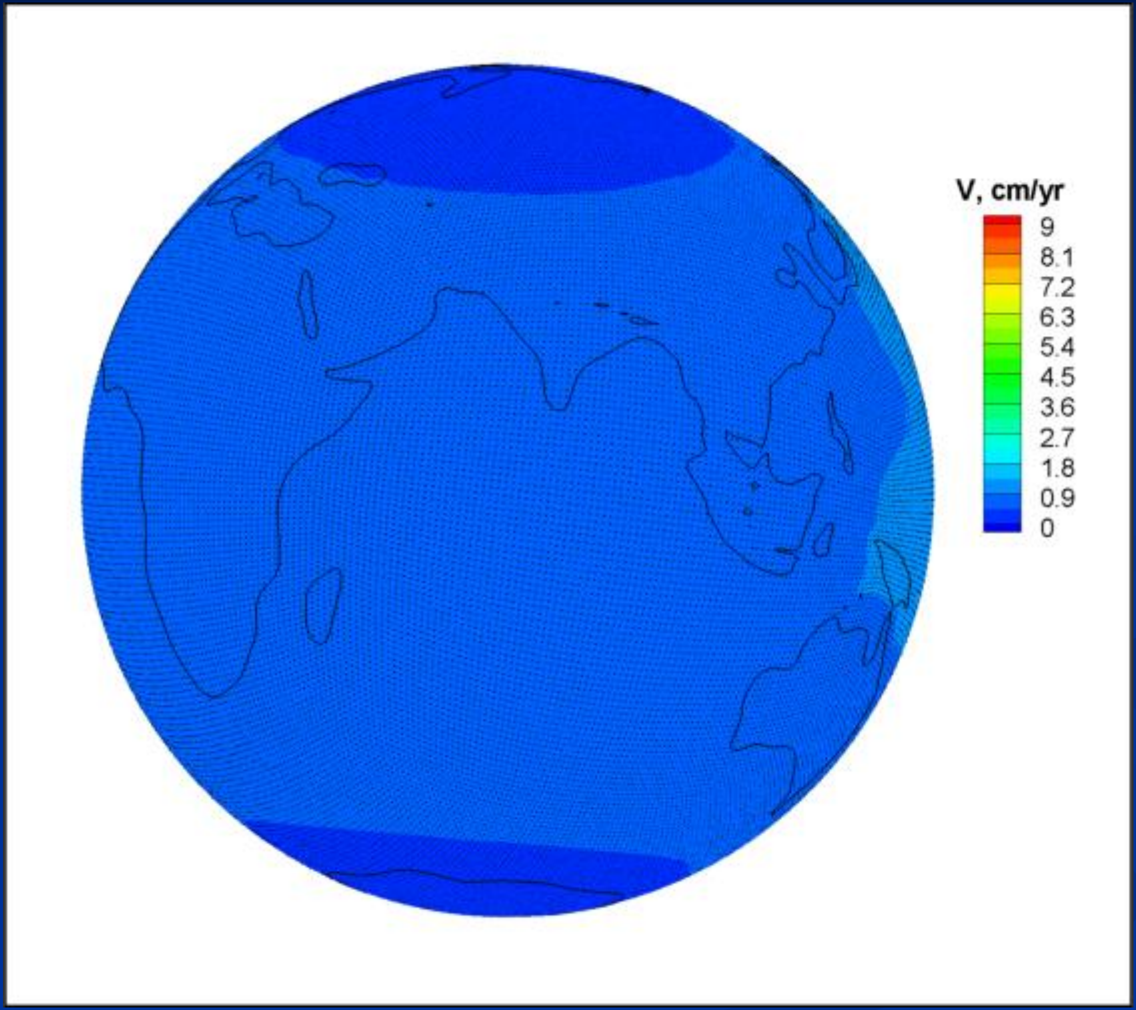

Friction at boundaries 0.1 (Smax=150 MPa)

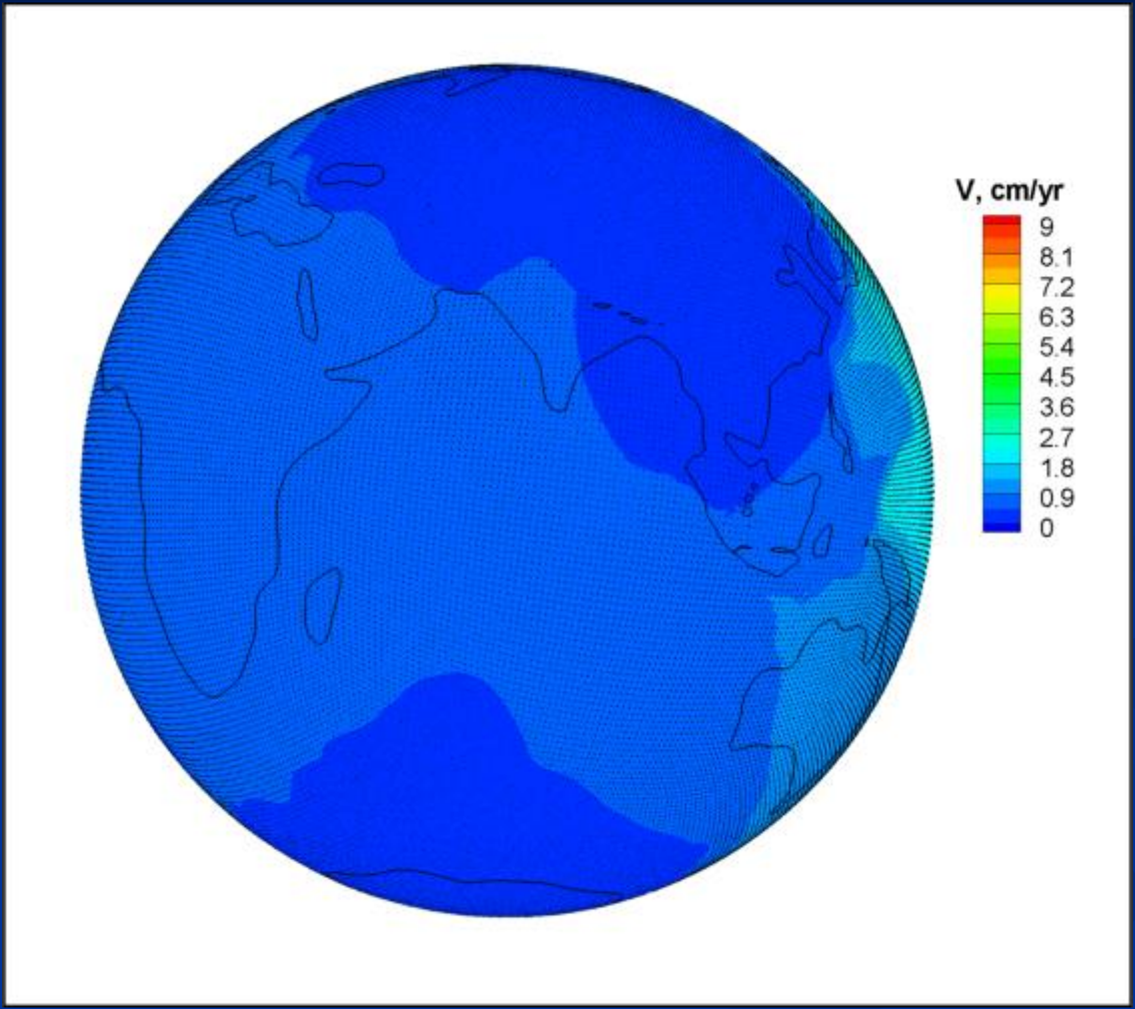

much too low velocities

Friction at boundaries 0.05 (Smax=75 MPa)

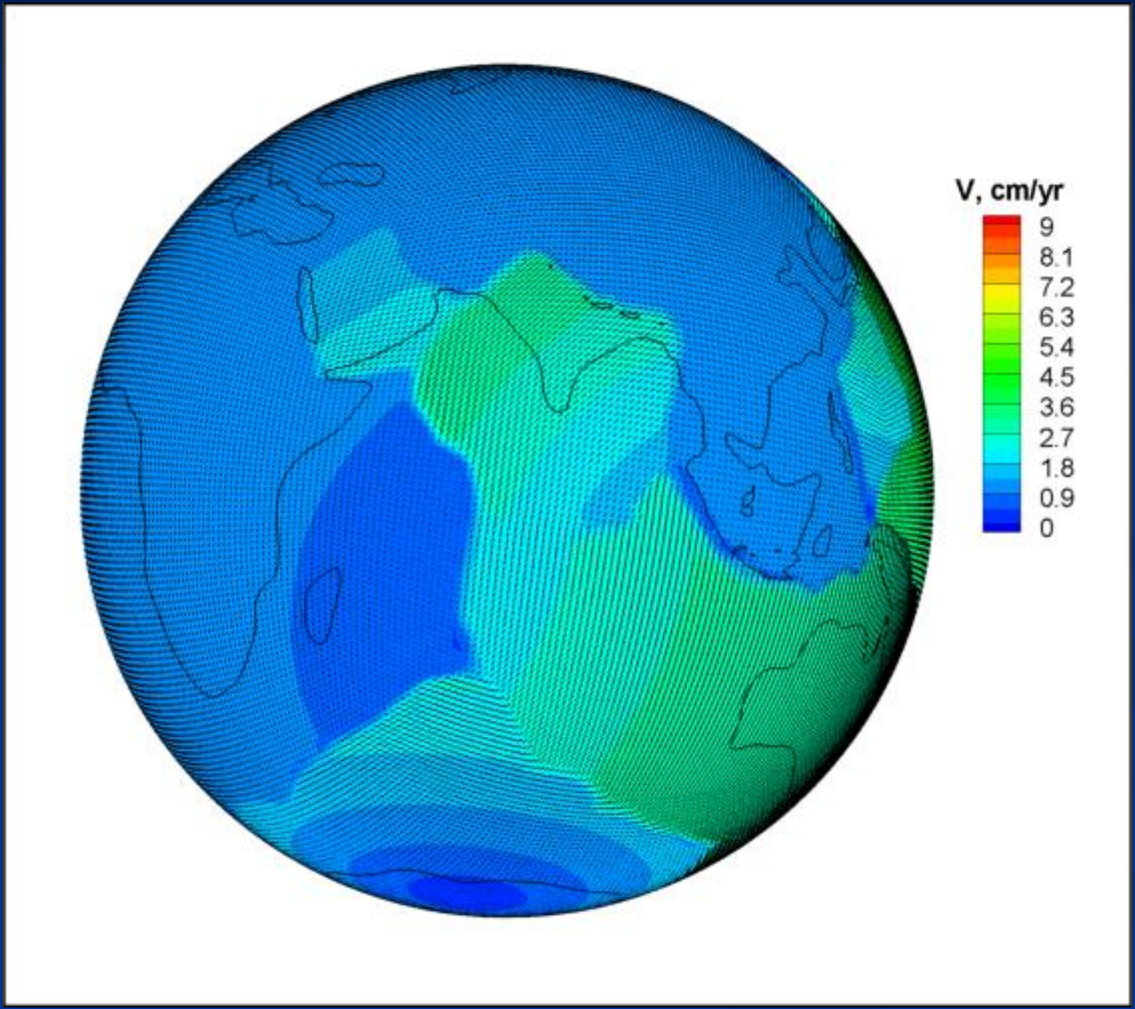

too low velocities

Friction at boundaries 0.02 (Smax= 30 MPa)

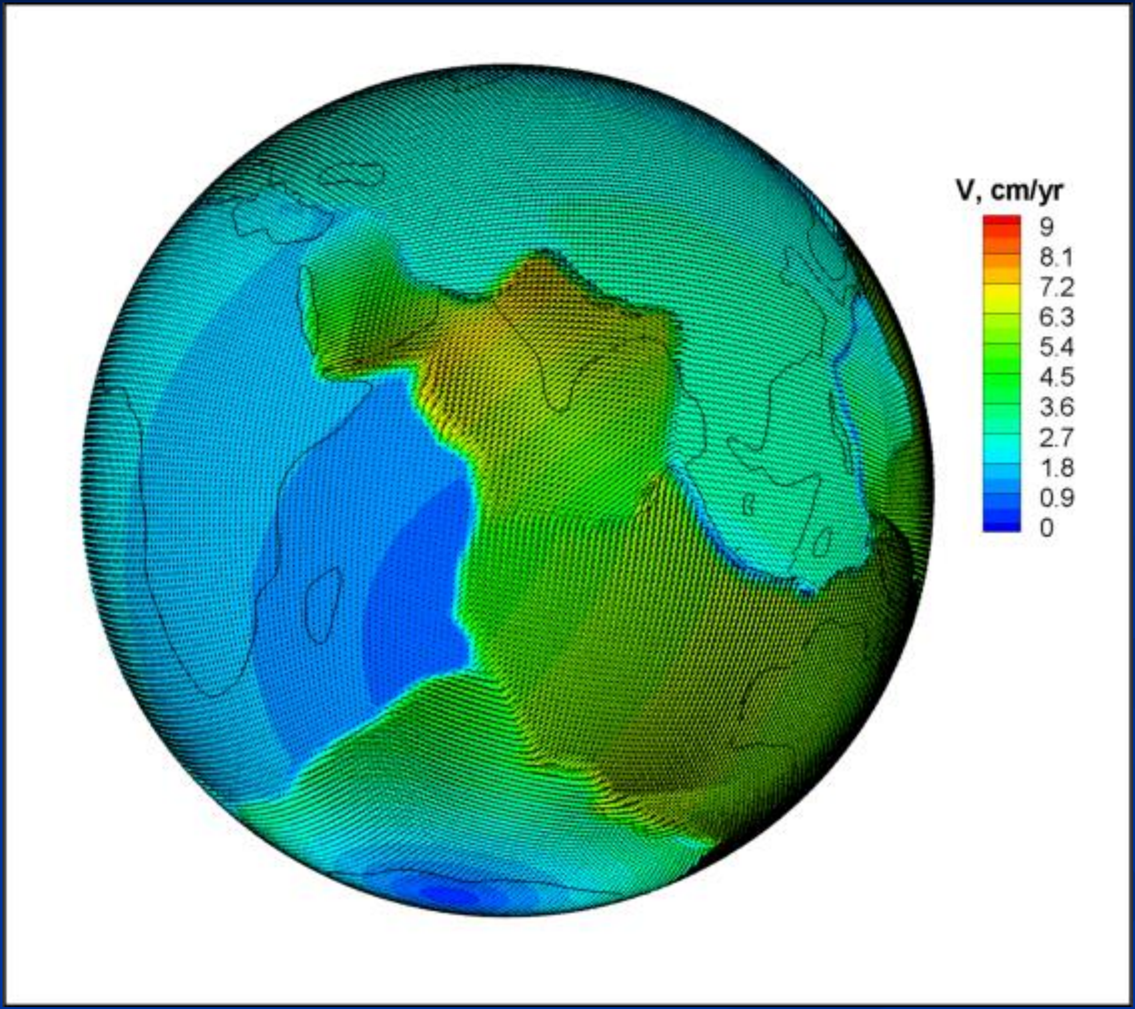

about right magnitudes of velocities

Friction at boundaries 0.01 (Smax= 15 MPa)

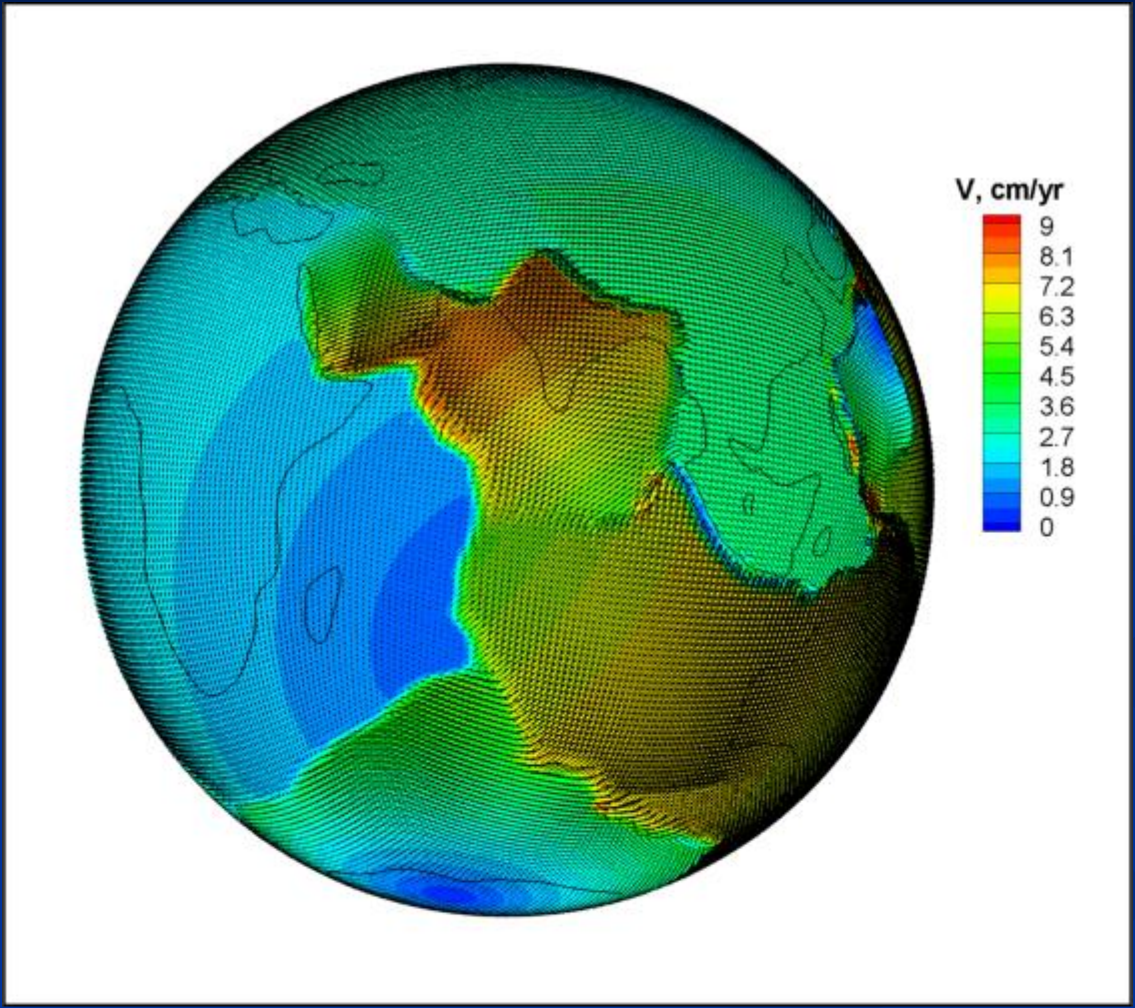

too high velocities

Point 2

Strength (friction) at plate boundaries must be very low (<0.02), much lower than measured friction for any dry rock (>0.1)

$$\mu_e = \mu \cdot (1 - P_{fl} / \sigma_n)$$

No high pressure fluid=no plate tectonics

Plate velocities in NNR reference frame

Model

Tp=1300°C,

lith: dry olivine;

asth: 1000 ppm H/Si in olivine, n=3.8

Plate bound. friction:

Subd. zones 0.01-0.03, other 0.05-0.15

misfit=0.25 (0.36 previous best by Conrad and Lithgow-Bertelloni, 2004)

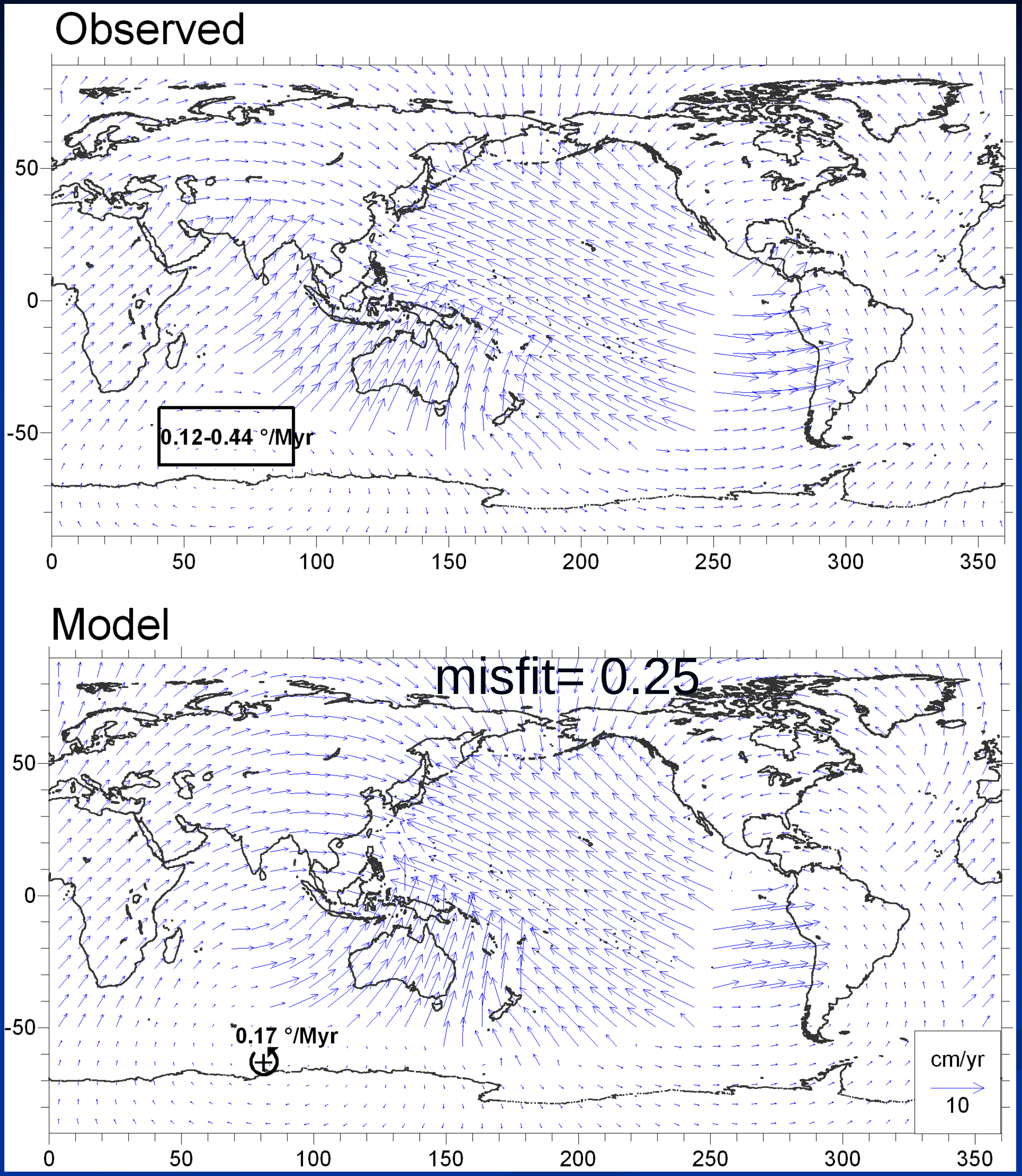

Point 3

The current views on the rheology and water content in the upper mantle are consistent with the observed plate velocities, if the stress exponent in the wet olivine rheology is pushed to the highest experimentally allowed values (3.7-3.8)